X-644-71-204
PREPRINT

NASA TM X- 65594

A COMPARATIVE GEOLOGIC STUDY OF SPACECRAFT AND AIRCRAFT IMAGERY

H. W. BLODGET

MAY 1971

GSFC — GODDARD SPACE FLIGHT CENTER
GREENBELT, MARYLAND

X-644-71-204

A COMPARATIVE GEOLOGIC STUDY

OF

SPACECRAFT AND AIRCRAFT IMAGERY

H. W. Blodget
Planetology Branch

May 1971

GODDARD SPACE FLIGHT CENTER
Greenbelt, Maryland

A COMPARATIVE GEOLOGIC STUDY OF SPACECRAFT AND AIRCRAFT IMAGERY

H. W. Blodget
Planetology Branch

ABSTRACT

A comparative study of five areas of northwest Saudi Arabia was conducted using five scales (1:18 million to 1:60,000) and types of imagery, and employing standard photo interpretation techniques. Results indicate that each type imagery is uniquely suited for investigation of a specific class of geologic problem. For study of small geologic detail and construction of precise maps, aerial photography is unexcelled. Mosaics permit extrapolation of inferences from individual photographs to larger areas, but with loss of detail. Orbital color photography appears to combine many advantages of mosaics and air photographs, for despite its low ground resolution, it is clearly valuable for studying regions of sub-continental size. When rectified, resolution on synoptic photographs is degraded, but the resultant near-vertical projection enables more accurate correlation of data between the unrectified photography and standard geologic map formats. Orbital scan-type imagery has very low ground resolution and may not be directly useful in geologic research. It does, however, provide a useful view of continental and intercontinental structural relationships. The various methods of remote sensing discussed are thus complementary rather than competitive, and can advantageously be utilized together in regional geologic investigations.

CONTENTS

PRECEDING PAGE BLANK NOT FILMED

CONTENTS (Continued)

ILLUSTRATIONS

TABLE

ACKNOWLEDGEMENTS

This investigation was accomplished with the kind cooperation and assistance of many individuals and organizations. I am especially grateful to Dr. P. D. Lowman, Jr. for stimulating discussions of orbital photography and for contributing valuable advice during the development of the study. Professor G. Teleki critically reviewed the manuscript and provided many valuable suggestions. Discussions of aircraft photography and mapping of Saudi Arabia with Mr. F. X. Lopez of the U.S. Geological Survey provided invaluable assistance in selecting the large scale areas of study. Mr. E. Sherkarchi of the U.S. Bureau of Mines provided the rectified orbital photo negative of the northern Red Sea Area. Finally, thanks are due to astronauts C. Conrad and R. Gordon, whose interest and diligence in conducting the NASA Terrain Photography Experiment provided the excellent Gemini 11 photographs.

This paper is modified from a Master of Science thesis submitted to the Department of Geology of The George Washington University.

A COMPARATIVE GEOLOGIC STUDY OF SPACECRAFT AND AIRCRAFT IMAGERY

INTRODUCTION

The objective of this study is to compare different types of presently available photographic imagery from spacecraft and aircraft in order to determine the advantages and limitations of each for identifying geologic features. This comparison is in turn intended to define the image characteristics best suited for solving specific problems. In addition, the study establishes approximate limits to the extent to which orbital photography can substitute for better but unavailable aerial photography or data from ground surveys.

Prior to 1960, several hundred photographs had been obtained from orbital altitudes by means of sounding rockets such as the V-2, Aerobee and Viking. Orbital imagery, however, did not become available until the launching of Tiros I in April 1960 (Lowman, 1964). Since that time, millions of individual pictures of the earth have been returned by electrical transmission of sensor recorded data in various spectral ranges or by film recovery. The vast majority have been transmitted by the various weather satellites, and these, being intended for meteorological use, have extremely low resolution. The various synoptic terrain photography experiments carried on the manned Mercury, Gemini and Apollo flights, however, have provided over 3,500 high quality photographs usable for geologic study.

Preliminary investigations have demonstrated the potential utility of synoptic photography in solving specific problems (Wobber, 1967, Abdel-Gawad, 1969, Merifield, et al, 1969, Lowman, 1969, and others); however, only limited investigations have been undertaken to compare the utility of orbital to aerial photography. To the author's knowledge, the work of Amsbury (1969) is the most comprehensive to date. Although this study was well designed for its stated purpose, it did not use the most representative imagery generally available for the smaller scales investigated. The interpreted synoptic photography was taken on the unmanned Apollo 6 mission which had a fuel allotment to permit near-vertical photography. The vast majority of available orbital altitude imagery has been taken at varying degrees of obliquity, and thus requires some rectification with inherent resolution degradation. Secondly, the 1:250,000 scale aerial photography was obtained with a specifically selected photographic system that did not produce the inherent patch-work appearance typical of air photo mosaics. On the other hand, a single 1:250,000 standard aircraft mosaic would cover a much larger area than the photograph used by Amsbury, and could perhaps in itself have permitted recognition of the structure-controlled alignment

noted, thus negating the single example of a unique advantage of the space photography described.

The study of Gemini photography by Lowman (1969) included a comparison of orbital and aerial photography. However, this comparison was not directed specifically to geologic applications; greatest stress was on general features of both types of photography, such as coverage and ease of dissemination.

It is clear, then, that despite previous work, there is still need for a comparison of the geologic utility of orbital and aerial photography. The purpose of this study is to meet that need by geologic study of imagery from spacecraft and aircraft with an extremely wide range of scale and resolution.

IMAGERY USED AND METHOD OF INVESTIGATION

This comparative study was made using five different scales and types of imagery taken over parts of northwest Saudi Arabia. These include: 1:60,000 aircraft photographs, 1:250,000 aircraft photo index mosaics, a 1:1,000,000 enlarged and rectified space photograph, a variable scale 7.5 × 7.5 inch (19 × 19 cm) color enlargement of the original space photograph, and a variable scale (smaller than 1:15,000,000) black and white Nimbus III high resolution infrared image reproduction.

The 1:60,000 aircraft photography used in this study was originally obtained for a joint geological mapping program sponsored by the U.S. Geological Survey and the Kingdom of Saudi Arabia. The photographs selected for this report were taken during 1956 and 1957 with a Fairchild T-11 camera equipped with a 6 inch (154 mm) focal length Bausch and Lomb Metrogon lens flown at 30,000 feet (9150 meters), and taken with 60 percent overlap and 30 percent sidelap.

The photo mosaics used are part of a series of 89 mosaics constructed primarily to provide a location index for all of the photography taken for the Western Shield Area photo project. Each mosaic covers slightly more than one degree on a side, and the 1:60,000 coverage included within a one degree unit was taken in 14 sidelapping flight lines, each containing 18 overlapping photographs. The mosaics were constructed by placing all the aircraft photographs within the one degree units in perspective, and photographing each group at a reduced 1:250,000 scale.

The 1:1,000,000 Gemini 11 photograph (S66-54644) was produced by optically rectifying the original oblique photograph, which was 15° 57.5' off nadir, into the horizontal plane and enlarging it to the desired scale. The rectification was done by the Raytheon/Autometric company for the U.S. Bureau of Mines; the

system used, however, has two major limitations. First, compensations can not be made for the curvature of the earth's surface, so the greater the obliquity, the less reliable is the photo base. Although any oblique photograph can be rectified, at least in part, it is recommended that the tilt angle be kept less than 35 degrees off vertical to obtain resolution acceptable for most general mapping purposes (Mac Kallor, 1968). Secondly, rectification can currently only be accomplished in the black and white format, thus losing the advantages of color in the unrectified photos. In spite of these limitations, the rectified photography is accurate enough to greatly facilitate correlating data between the synoptic photography and published base map (Dalrymple, 1970).

The original Gemini photograph was taken on September 14, 1966 as part of the Synoptic Terrain Photography experiment. The photo was made on Eastman Kodak Ektachrome (S0 368) film with a 70 mm modified Hasselblad Super Wide C camera equipped with a wide angle 38 mm focal length Zeiss Bigon lens and haze filter, and was taken from an altitude of 220 nautical miles (400 km). The camera setting was f 4.5 at 1/250 second. The camera was hand held, and no fuel was allotted for spacecraft orientation, so vertical imagery could not be obtained, resulting in inherent photo scale decrease toward the horizon (see Figure 2). Photograph S66-54895, referred to in the discussion of area 4, was also taken on the Gemini 11 mission on the same film type. This photo, however, was taken at an altitude of 160 nautical miles (290 km) with the specially designed J. A. Maurer 70 mm Space Camera, equipped with an 80 mm focal length Xenotar lens. The camera setting was f 2.8 at 1/250 second. The degree of obliquity has not been calculated, but is more nearly vertical than photo S66-54644.

The variable scale (smaller than 1:15,000,000) Nimbus III day time high resolution infrared imagery used in this study is an enlargement of the original 70 mm imagery strip constructed from reflected data in the near infrared (0.7 - 1.3 mu) obtained during horizon to horizon radiometer scans. The spacecraft radiometer mechanism includes a scanner which rotates continuously in one direction at 48 rpm. While the scanner is pointed away from the earth, the spacecraft moves forward just enough so that the next scan is contiguous with the first (Cherrix and Allison, 1969).

This comparative study was initiated with a description of the very small scale Nimbus III imagery (Figure 1). The great areal coverage and poor resolution allowed recognition of only extremely large geological features; thus, interpretation of this picture permits the subsequent larger scale photographs to be interpreted in an intercontinental context. Next geologic maps were constructed for the unrectified color enlargement of photo S66-54644 (Figure 2), so that the subsequently discussed larger scale imagery could be conveniently located. These maps were originally drawn as overlays to the color photo but are here

included as photo copies for convenience of presentation (Figure 2). After establishing the regional setting, five specific smaller areas were individually interpreted and discussed in respect to the 1:60,000, 1:250,000, 1:1,000,000 and unrectified color imagery. The areas were originally selected at the 1:60,000 scale, because they included interesting but different geologic features, and also exhibited tonal contrasts between different adjoining lithologies. The discussions include duly referenced data from the literature and published maps as well as detailed interpretations made directly from the imagery. Resolution for each of the specific format scales was measured with a 6 x tube magnifier with photo reticle (0.0005 ft. and 0.1 mm) graduated scales. This instrument is accurate to 0.05 mm in areas of moderate tonal contrast and slightly better in high contrast areas. Resolution within specific imagery was always measured across linear features of highest tonal contrast, such as a light-colored alluvium filled wadi cutting a dark lithology. This produces a higher resolution measurement than the effective resolution which is the general standard (Amsbury, 1969, et al). Because of the almost complete absence of metric surface control on this imagery, effective resolution can not be reliably determined, but the maximum resolution similarly determined on the various scale imagery is considered adequate to make quantitative comparisons between the imagery.

Overlays were constructed for each of the 1:60,000 photo sets to illustrate the detailed geologic features shown at this scale. DuPont 0.004 inch matte surface Cronaflex reproduction film was selected as the overlay base because of its resistance to wrinkling and shrinkage with normal handling. Thus, the overlay can be easily registered on the imagery as required. Best illumination for this work is obtained when the light source originated from below; thus, the photographs were placed on a light table so that all reflectance, which is inherent with exterior light sources, is eliminated. Each of the 1:60,000 photo sets had some overlap or sidelap, and the resultant stereoscopic coverage was fully utilized. Stereoscopic viewing proved particularly useful where relief was low and the lithologic contrasts were gradational. A Wild ST 4 mirror stereoscope with accessory 3 x and 8 x occulars was used for all stereoscopic viewing.

Upon completion of the 1:60,000 geologic photo area description, the more distinctive geologic features were examined at succeedingly smaller scales and degradation of recognition ability was recorded in respect to resolution decrease. Conversely, however, with decrease in resolution of the imagery used, field of view increased to permit recognition of the regional geology. The results of the five area investigations are compared and reported in the conclusion.

NIMBUS IMAGERY

A complete comparative study of various scale photography should include the very small scale imagery obtained primarily for meteorological investigations. Several earth-orbiting weather satellites have been launched to date carrying various radiometer and television camera combinations (Nordberg, 1970). Of these, qualitative studies suggest that the daytime high resolution radiometer imagery of the reflected near-infrared range (0.7 to 1.3 microns) produces the greatest geologic detail. Figure 1, an enlargement made from the Nimbus III high resolution infrared (HRIR) imagery clearly shows the major structural provinces of the central and western Arabian peninsula as defined by Powers, et al (1966).

Regional Geology

The Arabian shield forms the western portion of the Arabian peninsula and extends from the Gulf of Aqaba on the north to the Gulf of Aden in the south. For most of geologic history, this structural unit formed an eastern projection of the Nubian shield, but during the Tertiary it was separated from Africa by Red Sea rifting. The typical parallel structure lineations formed by rifting mechanisms is exhibited by the subparallelism of the Red Sea coasts, and is clearly discernible even at the compressed margin of the HRIR imagery. On Figure 1, the Arabian shield includes the dark mottled tones of the western third of the peninsula. This extensive area has been tectonically stable since the Precambrian and consists mainly of igneous and metamorphic rocks which are locally overlain by Cenozoic volcanics and Quaternary alluvial and eolian sediments. Some of the larger volcanic and sedimentary surfaces can be distinguished by their respective dark and light tonal characteristics on this imagery and are correlable with the existing published maps (Anon., 1966).

The shield area is bordered by the Interior homocline, a roughly 400 kilometer-wide belt of sedimentary strata which dip gently away from the shield. The beds consist variously of limestone, shale and sandstone, and range in age from Cambrian to Tertiary. Differential erosion and subsequent deposition of alluvial and eolian sediments in the topographically lower areas has produced the stripe-like pattern which can best be recognized in the area of the central Arabian arch. In the north and south, the homocline is in part covered by the extensive wind-blown sands of the An Nafud and Ar Rub al Khali respectively. The southern-most unit of the homocline, the Hadramawt plateau, is located between the southern Arabian shield and the Rub al Khali. This topographically high, dissected plateau consists of generally northward dipping limestone, shale and marl strata, and is characterized by medium grey hues on the imagery. The Wadi Hadramawt traverses the plateau in a generally east-west direction and is the dominant drainage system

on the plateau. The trunk of the wadi appears as a poorly defined thin sinuous line. Recognition of several of the major wadi branches is suggested, but resolution is below the limit of confirmation.

The Interior homocline is bordered by the Interior platform. The division between these two structural units is marked by the hinge line created by a break in slope between the slightly dipping strata of the homocline and the nearly flat-lying beds of the platform. The southern borders can not be defined with certainty on the HRIR imagery.

The configuration shown for the Rub al Khali basin, as defined in the literature (Powers, et al, 1966) is based on subsurface data. Although the structure of this area can not be determined from the imagery, the areal extent of the basin is characterized by the light toned areas of eolian and less commonly, alluvial materials deposited on the topographically low, flat surfaces. These surfaces, however, can not be distinguished from similar surfaces existing on some of the locally adjoining portions of the Interior platform.

The structural units which form the eastern-most Arabian peninsula can not be clearly identified because of the degree of imagery distortion at the margins of the horizon to horizon scan (Cherrix and Allison, 1969). The borders of the units plotted in this area are thus of limited reliability.

Resolution

Variability of scale and resolution over the image area is caused by a combination of earth curvature and scanning mechanics, and results in the images being greatly compressed on the east and west margins. Thus, in general practice, regional geologic investigations using these photo reproductions should avoid using the outer 15 percent of each strip. Observing this constraint on the 2.77 standard photo enlargement of the original 70 mm imagery strip, scale is computed to be approximately 1:17,000,000 in the east-west direction and 1:16,000,000 in the north-south direction across the Arabian peninsula. Maximum resolution determined in the high tonal contrast areas of the Central Arabian arch in central Saudi Arabia is computed to be 4.8 × 5.2 miles (7.7 × 8.3 km). On this imagery, the standard aircraft photographs would plot as an area slightly less than 1 mm^2 and thus would be below the effective resolution of the imagery. The 1:250,000 index mosaics each include an area of approximately 4250 square miles (11,000 km^2) which plots as an area of about 5 mm^2 in northwest Saudi Arabia. Those mosaics which include extended, sharply contrasting contacts such as light-colored sandstone against large basalt extrusives or coastlines can be correlated in a very generalized way in respect to those contacts. Almost none of the smaller features recognizable on the Nimbus III imagery, however, can be

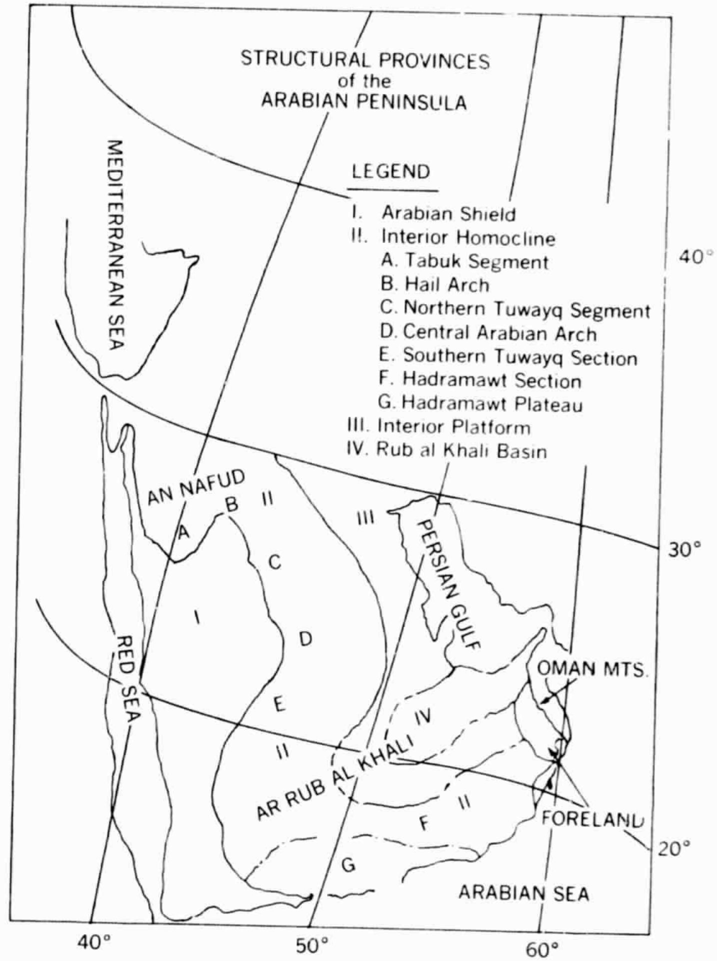

NIMBUS III HRIR DAYTIME ORBIT 711 6 JUNE 1969
ASIA MINOR

Figure 1. Structural Provinces of the Arabian Peninsula Visible on Nimbus HRIR Imagery

recognized within the field of the mosaic alone. The rectified orbital photography on the 1:1,000,000 scale provides a much wider field of view, and it is possible to correlate all the coastlines of the northern Red Sea, Sinai and eastern Mediterranean areas, the outline of the light-colored western portion of An Nafud in contrast with the pre-Tertiary consolidated sediments, and the northern Shield-Interior homocline contact, as well as to partly identify portions of the larger basalt extrusives and Quaternary deposits.

It is clear that major structural provinces can be recognized at the small scale of the Nimbus III HRIR imagery. These photos thus provide a tool for studying the inter-relationship of major structural units within systems of subcontinental magnitude, and for investigating even larger intercontinental structural relationships. The scale and resolution of the HRIR imagery, though much too small to be used in general mapping, does provide a valuable supplement to standard geologic mapping techniques, for it shows how the larger-scale mapped structure are related to the regional tectonic system.

GEMINI PHOTOGRAPH S66-54644

The African Rift valley system and its northern extension into the middle east were high priority targets for the Gemini and Apollo terrain photography experiment (Lowman, 1969). Toward attaining this objective, numerous cloud-free photographs of the northern Red Sea area were obtained during several Gemini and earth-orbital Apollo flights. Photograph S66-54644, however, was specifically selected for this study because of its wide areal coverage and strong definition of contrasting lithologic units. In addition, this particular photograph is one of a set of three which have been geometrically corrected by the Raytheon/Autometric Company for the U.S. Bureau of Mines, and is conveniently available in the rectified format at both 1:1,000,000 and 1:2,000,000 scales. Although not photogrammetrically reliable, the rectified imagery provides an excellent base for geologic map compilation when used in conjunction with existing geologic maps and the unrectified 70 mm color enlargements.

Photograph S66-54644 was taken by Astronauts Conrad and Gordon on September 14, 1966 during the 26th revolution of their Gemini 11 spacecraft. On orbits 26 and 27, the spacecraft was placed in high elliptical orbit (apogee 740 nautical miles - 1340 km; perigee 160 nautical miles - 290 km) for engineering studies. During this maneuver photographs were taken from the highest altitudes attained on manned orbit to that date, and these provided some of the most detailed large area coverage obtained on any of the manned orbital flights. Photograph S66-54644 was taken from an altitude of 220 nautical miles (400 km) with a 70 mm modified Hasselblad camera as previously described. A 7.5 × 7.5 inch (19 ×

19 cm) enlargement of this exposure is shown on Figure 2A, and the area of coverage is indicated on Figure 2B.

This photograph includes four major lithologic groups which can be mapped with varying facility. These include: Quaternary to Recent sediments, Tertiary to Recent volcanics, Cambrian to Tertiary sedimentary rocks and Precambrian rocks. Each of these units can be generally identified by a combination of both color and surface texture, however, local differences are at times so subtle on orbital photographs that serious mapping, even at this scale, should be supplemented by available geological maps and any other sources of information including aerial photography. The geologic map constructed for this synoptic photograph (Figure 2B) was developed with the use of the referenced sources.

The Precambrian shield rocks can, with minor exceptions, be delineated on the synoptic photography by their distinct moderately dark color combined with massive weathering textural characteristics. In the north, these generally dark rocks are locally intruded by peralkaline granite stocks, identifiable by their subcircular shape and light brown color. As previously discussed, prior to Red Sea rifting the Arabian shield formed the eastern portion of the single Arabo-Nubian shield complex. The photographic similarity of the related rock types on opposite sides of the Red Sea can easily be recognized on this single synoptic photograph.

In addition to very generalized lithologic correlation, one can identify linear features which are not shown on the existing geologic maps; these are particularly numerous in the Precambrian outcrop areas. This does not necessarily imply that these structures were not recognized by previous workers; it is likely that many linear structures, such as Precambrian fracture zones, are so numerous that only those which appear most prominent in the field could be conveniently plotted without causing undue congestion even at 1:500,000 scale. For this same reason, structural linears have not been plotted on Figure 2B, but they are discussed in the individual aircraft photo descriptions.

The ability to recognize such regional structures and lithologic groups could be of great economic importance. Even without considering the conflicting theories concerning the structural origin of the Red Sea (Dubertret, 1970), it seems reasonable to assume that the abundant pre-rift and possibly rift-associated mineralization of Egypt (Said, 1962, p. 259-273) would have structural and mineralogical counterparts in the Arabian shield. This, in fact, has been suggested by Dadet, et al (1970) in their discussion of mineral occurrences near Umm Lajj, Saudi Arabia. If they are correct in this inference, then hyperaltitude photography might be used to rapidly plot and correlate trans-Red Sea fracturing and mineralization, in order to isolate the areas which warrant field investigation.

In constructing Figure 2B, all of the Phanerozoic sedimentary rocks older than Quaternary age were grouped together for graphic convenience into a single mapped unit. Further subdivision is possible and, in fact, all of the formations mapped at 1:2,000,000 scale can be delineated on this photograph. For uncongested presentation, however, only the Cambro-Ordovician sandstone (OЄur), which has an appearance similar to Quaternary sediments in both color and albedo, has been individually identified with a vertical striped pattern. Sedimentary rocks within this mapped unit, south of the northern Gulf of Aqaba, consist of lower Paleozoic sandstones having local shale interbeds and lenses. These beds dip basinward at an inclination which rarely exceeds one degree. Southward, to the northern border of the largest OЄur unit mapped, a subtle east-northeast trending, sub-parallel pattern is superimposed over the entire mapped unit. This strong directional trend appears to be controlled by unidirectional wind currents which dominate the area. These linear features are clearly visible on the 1:250,000 photo mosaics but can be located only with difficulty on the 1:60,000 aircraft photography. The negligible relief change across individual contacts make it difficult to determine, from the photography alone, whether the pattern results from erosion, deposition, or both (see area 1 text). The great areal coverage of synoptic photography has permitted identification of the hitherto unrecognized regional nature of this geologic phenomenon.

In the north, the sedimentary lithology consists predominantly of cherty chalk, limestone and marl (TKb), and is largely of lower Tertiary age (Anon. 1966).

Intermediate and basic volcanics of Tertiary to Recent age are the most easily distinguished lithology from orbital altitudes. These young, slightly weathered deposits are characteristically very dark in color and nearly always in sharp chromatic contrast with the adjacent lighter colored lithologic units regardless of age. The common presence of finger-like flow appendages around the main extrusive bodies and local identification of individual volcanoes can further substantiate the identification. Even with these very distinctive characteristics, there are a few areas where young volcanics can not be readily identified from their surroundings on orbital photography. One of these is at the margins of the eastern-most mapped volcanic unit, and the contact is especially obscure on the south (see Figure 2B). Here, where the volcanics overlie the Precambrian Halban andesite (Anon. 1963), the long period of weathering did not alter the andesitic surface sufficiently to make it distinguishable from the Cenozoic basalt-andesite (QTb) flows at the resolution of orbital photography. The dashed line probable contact was determined by comparing the mapped units on U.S. Geological Survey map I-270A to the rectified imagery at the 1:2,000,000 scale, then transferring the field mapped contact to the unrectified enlargement. On the basis of weathering alone, individual Cenozoic flows can be recognized and dated relative to each other on the higher resolution aircraft and mosaic imagery (see

area 4 description). It thus seems most probable that this contact, which appears so nebulous on the Gemini 11 enlargement, could be clearly defined on the 1:250,000 aircraft mosaic imagery.

The Quaternary to Recent sediments mapped include eolian and alluvial sand, silt, and rarely salt deposits, all of which exhibit a characteristic light tan to buff color on the photo. On the Red Sea coastal plain, and covering the floors of the widest wadis, the light colored alluvium is well defined and can commonly be identified on the basis of color alone. Within the Arabian shield area, however, local alluvium concentrations commonly fill topographic depressions. The larger of these deposits can be generally recognized on the photography, but can not always be distinguished from many light-colored igneous units in the Precambrian massif. The peralkaline granites in particular resemble the smaller alluvium-filled depressions in both color and areal extent. This difficulty indicates that orbital photographs, which emphasize color and albedo, must in some areas be supplemented, even for small scale mapping, by aerial photographs that can, because of their higher ground resolution, provide lithologic clues in the form of topographic details. For example, the peralkaline granites and Quaternary sediments discussed here are readily distinguished from each other on larger scale aerial photography by their strongly contrasting tonal and textural characteristics (see area 3 and 4 descriptions).

The largest eolian deposits mapped within this orbital photo area form the southwesternmost extension of the Nafud desert. This extensive sand body is by far the largest of the sand deserts of northern Saudi Arabia and includes about 30,000 square miles (75,000 km^2) of mapped eolian deposits. This lithology, however, can not always be distinguished by color and surface texture alone, from the adjacent Cambro-Ordovician Umm Sahm and Ram sandstones of similar color (vertical striped on Figure 2B to show its areal extent within the mapped lithologic unit). The upper unit, Umm Sahm, is a crossbedded sandstone which weathers to pinnacles and contains local shale lenses, while the lower Ram unit is a massive, strongly-jointed continental sandstone which weathers to distinctly rounded forms (Powers, et al, 1966). These distinctive-weathering units can be identified by their texture on the higher resolution aerial photographs and mosaics, however, the resolution on all synoptic photographs is below this recognition capability. The boundaries of the differentiated units shown on Figure 2B were determined in conjunction with published geologic maps and the 1:2,000,000 rectified imagery, and are considered to show more detail than indicated on the 1:2,000,000 geologic map alone.

Figure 2A. NASA Photo S66-54644

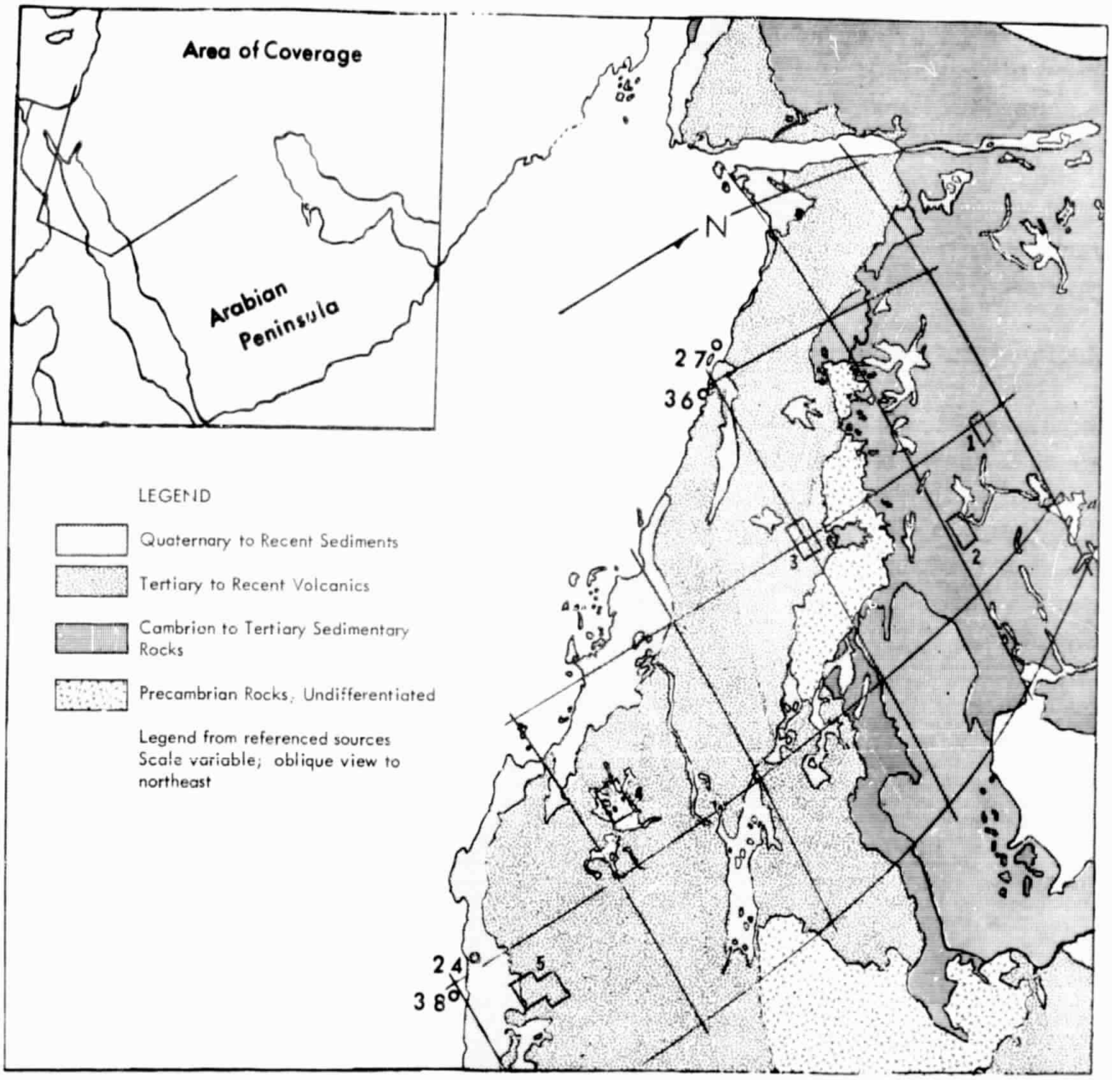

Figure 2B. Geologic Map of Northwest Saudi Arabia and Adjacent Areas, Constructed from NASA Photo S66-54644

AIRCRAFT PHOTO AREA 1

Photo area 1 consists of a three photo series including aircraft photos 20725, 20726 and 20727-WSA-133, and was initially selected (on index mosaic 17) because of the large, well defined, near-circular eroded dome structure located at the approximate center of the overlapping photo sequence, and to determine its visibility on various scale imagery. In addition, a moderately well defined dark shadow-like feature extends away from the northeast domal rim in an east-northeast direction. This is one of numerous dark elongate features typical of parts of northwestern Saudi Arabia which had been recognized earlier on orbital photo S66-54644.

Regional Geologic Setting

Stratigraphy—This photo series covers a 150 square mile (390 km^2) area located about 40 miles (65 km) east-northeast of the city of Tabuk. The surface has been mapped on the best available published map (Bramkamp, et al, 1963) as predominately shales and sandstones of the Tabuk formation (DSOt). In areas of deep erosion, Quaternary gravels (Qg) cover the floors of the major wadis.

Structure—Structurally the photo area forms part of the Interior homocline. This remarkably constant homocline regionally maintains a basinward dip which rarely exceeds one degree, and thus has the characteristics of an area of unusual tectonic stability. Significant structures do occur locally, as evidenced by the domal feature, but these appear to result from local uplift with no significant disturbance of adjacent parts of the momoclinal surface. The slight regional dip is northeast, and is probably influenced by the Sirhan-Turayf basin to the north (Powers, et al, 1966).

Interpretation of the 1:60,000 Aircraft Photography

The area included in this three photo set consists of two basic lithologies. The Tabuk formation (DSOt) is dominant and forms the major relief of the area. This unit, in the type locality, consists of approximately 3350 feet (1100 meters) of sandstone, which is generally fine-grained and in part silty and shaly and interbedded with shale beds. The sediments tend to become more argillaceous with depth, and terminate in a basal unit containing a few thin, irregular impure limestone horizons. The type section for this stratigraphic unit was compiled in several increments within 50 miles (80 km) of the city of Tabuk, so the photo area should not differ greatly from the type-area descriptions. Where the Tabuk formation has been deeply eroded, the wadis are floored by alluvial deposits which include sandstone and chert of local origin. Although only gravels are mapped in the immediate interest area at 1:500,000 scale, a finer grained lithology is also

evident on the aircraft photographs, similar to that mapped in nearby areas (Qs).

Drainage within the concentric rims of the eroded dome consists of a radial fan-like wadi system which merges into a singular trunk towards the west where it emerges through a breach in the southwest flank. This large trunk wadi could represent part of the pre-domal drainage pattern that was superimposed with only minor modification of its course. Drainage on the outer rim generally flows outward down the slope, sub-perpendicular to the rim and into the major arcuate stream beds to the north and south of the dome. Near breaches in the dome, however, the down-dip drainage goes directly into the major artery traversing the dome. The major arcuate wadis to the north and south of the dome form a local annular drainage pattern. They flow in a generally westward direction and coalesce with the main artery emerging from the domal interior at distances of one and two miles (1.6 and 3.2 km) respectively. The radial drainage characteristics appear to be limited to approximately two miles of the dome rim. Beyond this the drainage assumes a dendritic pattern which is locally modified by structural lineaments.

The dominant structural feature on this three photo set is the 3.5 mile (5.6 km) diameter eroded dome approximately centered on the strip. The discrete beds which form the elevated circular rim consist most likely of more highly indurated sandstone beds of the Tabuk formation. An alternative rim-forming lithology would seem unlikely due to the proximity of the type area. The underlying pre-Tabuk sediments, as determined from mapped outcrops in the west and from published stratigraphic sections, consist of about 2150 feet (650 meters) of Cambrian and Ordovician sandstone unconformably overlying the Precambrian basement (Bramkamp, et al, 1963 and Powers, et al, 1966). This thin section and lack of recorded evaporites in the area make the possibility of a salt diapir origin for this structure unlikely. On the other hand, even though no igneous activity is indicated on the regional stratigraphic section (Powers, et al, 1966, Plate 1), Bramkamp (1963) has mapped basalt (QTb) 30 miles (48 km) south of the dome.

A small arcuate anticlinal structure is superimposed on the south flank of the dome. This may be a pre-existing structure distorted by the dome-forming mechanism, but this interpretation seems unlikely in view of the generally simple regional structure. A more consistent explanation would be that the small anticlinal feature is directly related to the formation of the dome.

The major structural lineaments indicated on the 1:500,000 geologic map in the photo area do not appear to have great influence on the drainage pattern. In fact, several other segments of the main drainage, not coincident with mapped lineaments, appear to be straight for greater distances.

The "shadow" extending east-northeast from the northeast rim, which is so distinctive on the smaller scale photography, is barely discernible on the 1:60,000 aircraft photos and could easily remain unnoticed using only the larger scale imagery. The linear nature of the northern part of the shadow contact and its apparent initiation at the areas of greatest relief indicate that the nature of the shadow is wind controlled. At this preliminary stage of investigation, however, the originating mechanism is not fully understood.

The maximum resolution, measured in areas of highest tonal contrast, such as light colored alluvium deposited on a darkly-weathered outcrop, is 30 feet (9 meters); resolution in lower contrast areas decreases to 40 feet (12 meters). Resolution on these photographs is slightly poorer than on the other aircraft photographs studied. This appears to be due to the general tone darkness and a paucity of strongly contrasting lithologies. In constructing the overlay for the 1:60,000 air photographs (Figure 3), only drainage of 60 feet (18 meters) or larger was recorded.

Interpretation of 1:250,000 Index Mosaic 17

Index mosaic 17 of the western shield area, Saudi Arabia, includes the one degree area bounded by the 28 and 29 degree north latitude, and 37 and 38 degree east longitude graticules. Bedrock in the area is predominantly Tabuk (OSDt) sediments in outcrop which are locally overlain by gravels (Qg) and finer alluvial sediments (Qs) along the more broadly developed drainage arteries. A few minor eolian sand deposits (Qes) are mapped in the western quarter of the mosaic. Several residual outcrops of the uppermost member of the Tabuk formation, the Tawil sandstone member (Dtw), are scattered across the northern third of the mosaic area, and in the extreme northwest, one of these minor outcrops is unconformably overlain by two very small Cretaceous (Ka)-Tertiary (Tlc) outliers.

Within the small aircraft photo area, the concentric rims of the eroded dome strongly contrast the contiguous, nearly horizontal strata. The minor anticlinal feature on the south flank can be seen on the mosaic, but even under magnification, its total structure can not be distinguished. Although this structure is approximately 1 × 0.25 miles (1.6 × 0.4 km) in area, its structural character is masked by the dominant topography of the dome.

The major northwest-trending fault mapped across the northeast quarter of photo area by Bramkamp (1963), appears to be correlative with a sub-linear topographic high, and can not be recognized on the mosaic as a major fault trace with any degree of certainty. The second large fault indicated on the 1:500,000 published map, is located about 1 mile (1.6 km) west of the dome and trends in a general north-south direction. This structural unit is probably responsible for the

sub-linear drainage, but can not be clearly recognized on either scale photography with confidence. In fact, because of their straightness, the major east-west wadi, which traverses the dome, and several lesser intermittent stream beds are more distinctive than the mapped faults.

The most significant feature which can be identified much more easily on the mosaic than on the 1:60,000 photos is the dark east-northeast trending shadow-like feature mentioned earlier. The northern edge of the feature is clearly defined for a distance of about 12 miles (19 km), where it dissipates rapidly into a darker surface lithology and appears to terminate at a northwest trending, partially sand covered escarpment. The southern margin of the dark area is not well defined, but can be seen to have a more nearly easterly trend, that causes a slight broadening of the "shadow" toward the east. The dark area, which can be clearly identified on the northwestern part of the mosaic, can be correlated into the much larger pattern recognized on the earth orbital photography. The consistent, sub-parallel regional nature of the "shadow" trends on the smaller scale imagery, and the apparent common initiation of the shadows at areas of higher relief suggest that they are genetically related to the fairly consistent regional wind system of northwest Saudi Arabia (Holm, 1968). Although on a much larger scale, the dark areas appear similar to areas between sand streamers which, according to Smith (1965) may cross minor stream courses without interruption or deviation.

Maximum resolution, measured in the highest tonal contrast of the interest area, is determined to be 115 feet (35 meters). In areas of lower tonal contrast, resolution is reduced to 155 feet (50 meters).

<u>Interpretation of the 1:1,000,000 Rectified Orbital Photography</u>

The one thing that can be determined from the synoptic view which was unknown, even from the aircraft mosaic, is the extent of the distribution of sub-parallel "shadow" areas and apparently related elongate outcroppings. The combined occurrences are recognized over an area of nine square degrees on the rectified mosaic and probably extend still further east beyond the borders of the currently available synoptic photography. From the earth orbital photography, it has thus been determined that sub-parallel linear trends are superposed on the geology of much of northwest Saudi Arabia.

The immediate area of the three photo set can be identified on the rectified photograph with difficulty and must be accomplished by correlation with the major regional drainage and the distinctive "shadow" trends seen on the index mosaic. The primary reason for this difficulty is that foreshortening caused by the photo obliquity reduces the resolution toward the horizon, leaving only the largest

features readily discernible. In fact, within the aircraft photo area, only the dark area associated with the three mile wide dome could be identified with any degree of certainty, and this has a width of approximately 1.5 miles (2.4 km) (as measured on the index mosaic). The dome appears distorted on the rectified photograph because of the large photo angle and because of the low tonal contrast with its surroundings, is almost below recognition resolution at the 1:1,000,000 scale. It is, however, more easily identified on the unrectified color photography on which the resolution has not been degraded by the rectification process. Because of the low color contrast, this reasonably large structure would probably not have been identified by studying the space photo alone.

Ground resolution on the space photography increases proportionately in the direction of the sub-satellite point with maximum resolution obtained on vertical photographs.

Comparison of the Various Scale Imagery

The 1:60,000 aircraft photographs yield by far the greatest detail and are available with stereoscopic coverage. All the geologic units mapped by Bramkamp, et al (1963) in Area 1 can be identified, and some of these units can be subdivided. Some additional structural fracturing might be inferred from local straightness in the drainage system. The shadow-like feature which extends from the northeast rim of the dome could very easily go unnoticed on interpretations using this scale imagery alone.

Resolution at the 1:250,000 index mosaic scale is also adequate to distinguish units mapped on the largest scale published map (1:500,000), and some of these units can be subdivided. All of the drainage trends noted at 1:60,000 scale are recognized, and can be further observed in a more regional context. The major regional structure mapped by Bramkamp (1963) can generally be recognized, and possible additional regional zones of structural weakness might be inferred by local straightness in drainage. The distinctive dark shadow-like feature extending east-northeast away from the outer rim of the dome can be seen in its entirety at this scale, and also be recognized as being one of several similar features in the area.

Of the five areas studied, Area 1 is the farthest off nadir and is extremely difficult to recognize on the earth orbital photography in either the rectified or unrectified format. This inherent disadvantage of oblique orbital photography results in reduction of structural and lithologic detail toward the horizon. The dominant linear trend in photograph S66-54644 appears to be, in the area of the mosaic, roughly N 70° E. This might be taken for regional strike or a regional fracture pattern if no larger scale coverage were available. But study of the mosaic shows

FOLDOUT FRAME

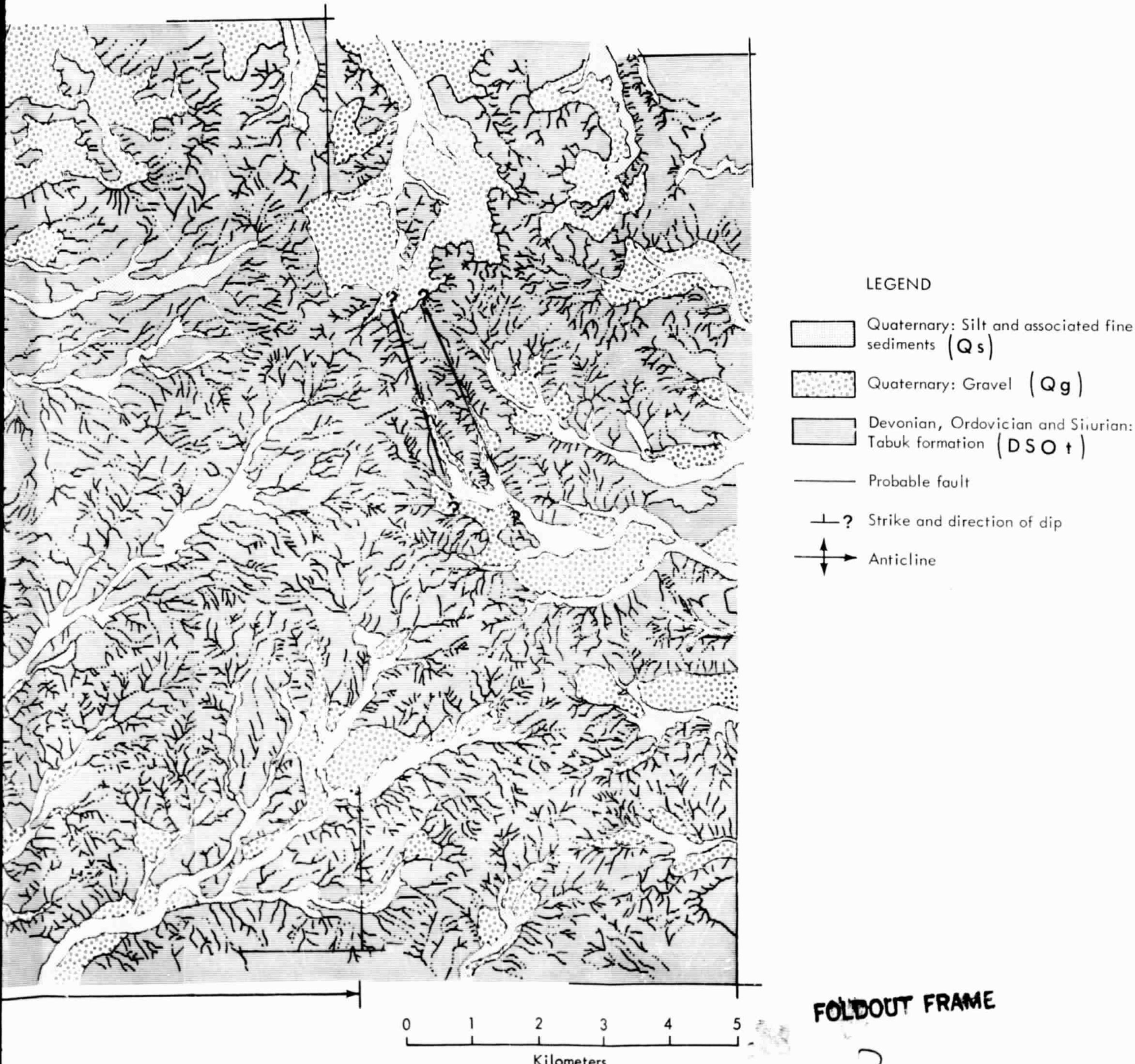

FOLDOUT FRAME

2

Figure 3. Area 1 Geologic Map – (Modified after Bramkamp, et al, 1963) – Based on Aircraft Photographs 20725, 20726 and 20727-WSA-133

this trend to be, as discussed previously, of probable eolian origin; the dominant fracture and local fold trends are in fact nearly perpendicular to the eolian features. This would not be apparent on the orbital photography, and demonstrates the necessity of supplemental larger scale photography for general geologic mapping.

AIRCRAFT PHOTO AREA 2

Area 2 consists of overlapping aircraft photo pair 15967 and 15968-WSA-96, and was initially selected (on index mosaic 17) to investigate a unique, intricate drainage pattern developed on a dark outcrop area and to determine its visibility on various scale imagery.

Regional Geologic Setting

Stratigraphy—These photos cover a 120 square mile (300 Km^2) area located approximately 72 miles (120 km) east-southeast of the city of Tabuk. The area has been mapped by Bramkamp, et al (1963) as consisting predominantly of shales and sandstones of the Tabuk formation (DSOt). Where the Tabuk formation has been deeply eroded by the main drainage arteries, Quaternary gravel (Qg) and silt (Qs) deposits commonly cover the wadi floors.

Structure—The area forms a part of the Tabuk segment of the Interior homocline. Thus, for a summary of the regional tectonics, the reader is referred to the structure description of Area 1, which is located about 75 miles (120 km) to the northwest.

Interpretation of the 1:60,000 Aircraft Photography

The area recorded by photographs 15967 and 15968-WSA-96 includes two basically different lithologies. The dominant strata, which are generally dark, nearly horizontal, and topographically higher, represent the Tabuk formation (DSOt) of Bramkamp (1963) within the immediate interest area. Where this unit has been deeply eroded, alluvial deposits of local derivation have been deposited over the lowest areas to form the floors and flood plains of the arterial wadi system.

In the type area (Powers, et al, 1966) the Tabuk formation consists of approximately 3350 feet (1100 meters) of sandstone that is generally fine grained and in part silty and shaly, interbedded with shale. The lithology tends to become more argillaceous with depth, and terminates below a basal unit made up of a few thin, irregular impure limestone horizons. The type section was compiled in several increments within 50 miles (85 km) of Tabuk, so this photo area should not differ

greatly from the type locality provided that lateral continuity persists as indicated.

The Tabuk formation within the immediate study area is characterized by a distinctive compound dendritic-parallel drainage pattern (Feldman, et al, 1968). The major arteries have developed a dendritic drainage system which includes several meanders, and the tributaries form a parallel overprint trending north-northwest. These tributaries are remarkably regular in trend and spacing. Directions in trend where reliably measurable range between N 19° W and N 25° W, and spacing between tributaries varies between 400 and 800 feet (120 to 240 meters) and average about 500 feet (150 meters) where the pattern is best developed. This regularity gives the surface a corrugated appearance, and suggests that the pattern developed on the near-horizontal strata, and is controlled by zones of structural weakness which are probably joints. Of the various lithologies in the Tabuk type section, this unit is most likely a sandstone rather than a shale, judging from the higher topographic position and rectilinear tributary drainage development (von Bandat, 1962, pp. 94-104). Where locally more indurated, the lithology ($OSDt_1$) has greater relief and supports a higher elevation drainage subsystem. This appears to be the remnant of an earlier drainage system which was altered by subsequent uplift and erosion of the less resistant strata.

A southeast dipping, northwest trending cigar-shaped structure, 8 miles (13 km) by 1.1 mile (1.8 km) in dimension, bisects photograph 15968-WSA-96, and terminates the well developed parallel drainage overprint on the east. The strata forming the margins of this body appear to dip steeply inward, forming a narrow southeast-plunging syncline. Although the relationship between this syncline and the adjacent structure is not immediately evident, its proximity and near-parallelism to the structure-controlled (?) drainage suggests formation by the same or related stresses. The uppermost strata of the northwest half of the syncline are dominated by a dark, erosion-resistant lithology which is in part, at least, responsible for the higher topographic position of this structural body. These beds dip southeastward below the strongly indurated sandstone strata ($DSOt_1$) discussed above. Although the syncline plunges below the surface, its outline is expressed on the overlying sandstone. The areas immediately above this structure ($DSOt_2$) support meandering drainage which is characteristically associated with the old age stage of an erosional cycle. This suggests that this drainage is the superimposed remnant of the earliest erosional cycle still evident in the immediate interest area.

From the evidence available, the following historical sequence is indicated for this area of aircraft photo coverage:

1. Sandstone was widely deposited in this part of the Tabuk basin.

2. The cigar-shaped syncline was formed.

   a. The structure is younger than the contiguous sediments because it influences the overlying sandstone to the southeast.

   b. The structure-forming mechanism directly affected the sandstone strata immediately to the west and was directly responsible for the closely spaced flexures and/or jointing controlling the drainage. This genetic relationship further provides a mechanism for the limited lateral development (see photo index 17) of the unidirectional structural trend.

3. The entire area was eroded to near base level and developed a characteristic old age meandering drainage system.

4. Slow epeirogenic uplift rejuvenated the streams but the meander pattern was retained on the surfaces most resistant to erosion ($OSDt_2$). A slow rate of uplift is indicated by the incised meander developed across the center of the strongly indurated structure.

5. The increased gradient created by the uplift caused the alteration of the arterial meanders into a dendritic pattern which was maintained through the final stages of slow uplift. ($OSDt_1$) represents an intermediate surface) and still forms the arteries of the current system.

6. The present tributaries are primarily under structural control and produce the parallel overprinting of the compound drainage system seen on the modern land surfaces.

Two major northwest-southeast trending faults cross the northeast corner of the photo area and have been mapped by Bramkamp, et al (1963). The western fault is 1.6 miles (2.7 km) northeast of and nearly parallel to the cigar-shaped structure previously discussed. This fracture is accentuated by that part of the drainage system which it controls, and can be extrapolated below the alluvium covering its northwest limit within the interest area. No correlable off-set beds are distinguishable so the magnitude of lateral displacement, if any exists, can not be determined. The eastern fault trends N 27° E and is more nearly parallel to the parallel drainage developed to the west. The significance of this relationship, if there is in fact any, can not be determined within the immediate interest area. The fault trace is recognizable throughout its extent across the area, but is not as well defined as the more westerly fault.

Maximum resolution determined in areas of high tonal contrast, such as fourth order tributaries on the dark patterned sandstone, is 20 feet (6 meters). In areas

of moderate contrast, however, such as the Quaternary alluvium, resolution is only 30 feet (9 meters).

Interpretation of 1:250,000 Index Mosaic 17

Index mosaic 17 of the western shield area, Saudi Arabia includes the one degree area bounded by the 28 and 29 degree north latitude, and 37 and 38 degree east longitude graticules. The geologic description of this mosaic was previously discussed in the Area 1 description.

The distinctive compound drainage pattern seen on the two air photographs just discussed is clearly discernible on the mosaic and is recognized as being restricted to this small area. The long narrow syncline can be identified by both tone and shape, however, the meanders which traverse the length of the structure exhibit poor tonal contrast and can best be recognized under magnification. The nature of this structure is difficult to determine on the mosaic, and thus the ability to infer the geologic evolution of the landscape from the 1:250,000 scale photography alone would be questionable. The fault pair which traverse the northeast corner of the study area can be easily traced as far north as wadi Abu Aradah, but from there northward the western fault is ill defined. Additional faults mapped by Bramkamp, et al, traverse the index mosaic in a generally north-northwest direction, and can be traced across the mosaic with varying degrees of reliability. Other straight arterial drainage, most notably wadi Najr, is suggestive of unmapped fractures. The regional mapped trend is probably not directly related to the parallel drainage of the study area, for if this were to be proposed, it would be difficult to explain restriction of this unique pattern to such a small area when the lithology throughout the area is considered to be fairly uniform.

This particular photo index is of additional interest because of the east-northeast trending shadow-like features in the northwest quarter, which were described earlier in the Area 1 description.

Maximum resolution determined in areas of high tonal contrast and linearity is measured to be 115 feet (37.5 meters). In areas of lower contrast, resolution is reduced to 155 feet (50 meters). These resolution determinations were measured on the same surface-type areas used to determine the 1:60,000 scale data.

Interpretation of the 1:1,000,000 Rectified Orbital Photography

The area included within the coverage of the aircraft photo pair can reliably be defined on the rectified orbital photograph in spite of the limited tonal contrast. Wadi al Kalbah traverses the northwest corner of the area and can be readily

identified by its linearity and association with the major rectilinear drainage pattern formed by wadis Qalibah, Abu Ardah, Fajir and others (Bramkamp, et al, 1963). Once the area is located in respect to this wadi, the general outline of the darker tone patterned sandstone and lighter toned alluvial deposits in the southeastern third of Area 2 can be identified. The boundaries of the specific units are not sharply defined, but in collaboration with enlarged, unrectified color photographs, all of the major lithologic units mapped by Bramkamp at 1:500,000 scale can be identified, as well as the outline of the uniquely patterned sandstone body and the cigar-shaped structure. Tributary drainage within these units, however, is well below the limits of resolution.

Resolution in the area of highest tonal contrast, that is, across the narrowest width of Wadi al Kalbah discernible on the imagery, is 975 feet (300 meters). The resolution falls off so rapidly with decrease in tonal contrast and meaningful quantitative measurements can not be made.

Comparison of the Various Scale Imagery

The 1:60,000 scale aircraft photographs yield by far the greatest detail and are available with stereoscopic coverage. Conversely, however, they have the smallest field of view. All the major geologic units mapped by Bramkamp et al (1963) in Area 2 can be identified and, in addition, some of these units can be further subdivided on the basis of distinctive tone, texture and topography. Structures of small to intermediate size can be recognized and described, and detailed geologic interrelationships can be identified.

Resolution at the 1:250,000 scale of the photo index mosaic is also adequate to distinguish units on the largest scale published geologic map (1:500,000), and some of these units are also amenable to further subdivision. Anomalous conditions can be recognized but their relationship to contiguous geologic units can not be easily determined. Conversely, however, the much larger field encompassed in the mosaic permits the small interest area to be seen in the regional context. In the case at hand, the lithology hosting the distinctive, well defined composite drainage pattern is seen to be unique within the one degree field of view, which suggests that it is genetically related to a local structural mechanism or represents a unique lithology of very limited lateral distribution. In addition, unmapped structural trends can be inferred from the existence of local rectilinear drainage.

The resolution of the rectified hyperaltitude photography is adequate to permit identification of the aircraft photo area and to show its position within the regional tectonic framework. This image includes part of Saudi Arabia approximately twenty times greater than that covered by a single one degree air photo

mosaic. Thus, rather than only recognizing that the small area is a part of the Tabuk segment of the Interior homocline, the total area is viewed in respect to the adjacent Precambrian shield and its interrelationship with the Red Sea rifting of Tertiary age. At the same time, all of the major lithologic units mapped at 1:500,000 scale are correlable in collaboration with unrectified color orbital photographs. The latter provide color differences in addition to tonal difference recognition, permitting identification of numerous additional subtle geologic relationships not seen on the rectified image alone.

AIRCRAFT PHOTO AREA 3

Area 3 consists of overlapping aircraft photo pair 9353 and 9354-WSA-59, and was initially selected (on index mosaic 39) to compare the recognition of contrasting lithologies on various scale imagery. This photo area includes three distinctly different Precambrian petrographic units separated by sharp contacts, and this should permit nearly maximum recognition of contrasting rock types within the Arabian shield.

Regional Geologic Setting

Stratigraphy—The photo pair covers a 115 square mile (300 km^2) area located 70 miles (115 km) east of Ras al Azlam on the Red Sea coast. According to the best published geologic map (Brown, et al, 1963), rocks in this area are predominantly greenstone (gd), with minor areas of pink-red granite (gr) in the northwest and southwest corners, and an irregular intrusive in the south-central part of the photo area which is considered to be a light-colored granite (gm?). The area of probable pink-red granite (gp?) mapped in the northeast corner is difficult to distinguish from the greenstone lithology on aircraft photograph 9353-WSA-59 alone.

Structure—The Precambrian rocks form a part of the stable Arabian shield. Although the Arabian Precambrian rocks indicate major tectonic activity during their early history, they have been primarily influenced by epeirogenic movement during Phanerozoic time.

Interpretation of the 1:60,000 Aircraft Photography

The area recorded by photographs 9353 and 9354-WSA-59 includes two fundamentally different rock types. The light-toned, topographically lower areas which occur in the south-central part and western and northeast corners of the photo area are Precambrian granites. The darker, topographically high exposures covering the remainder of the area consist of greenstone of Precambrian age.

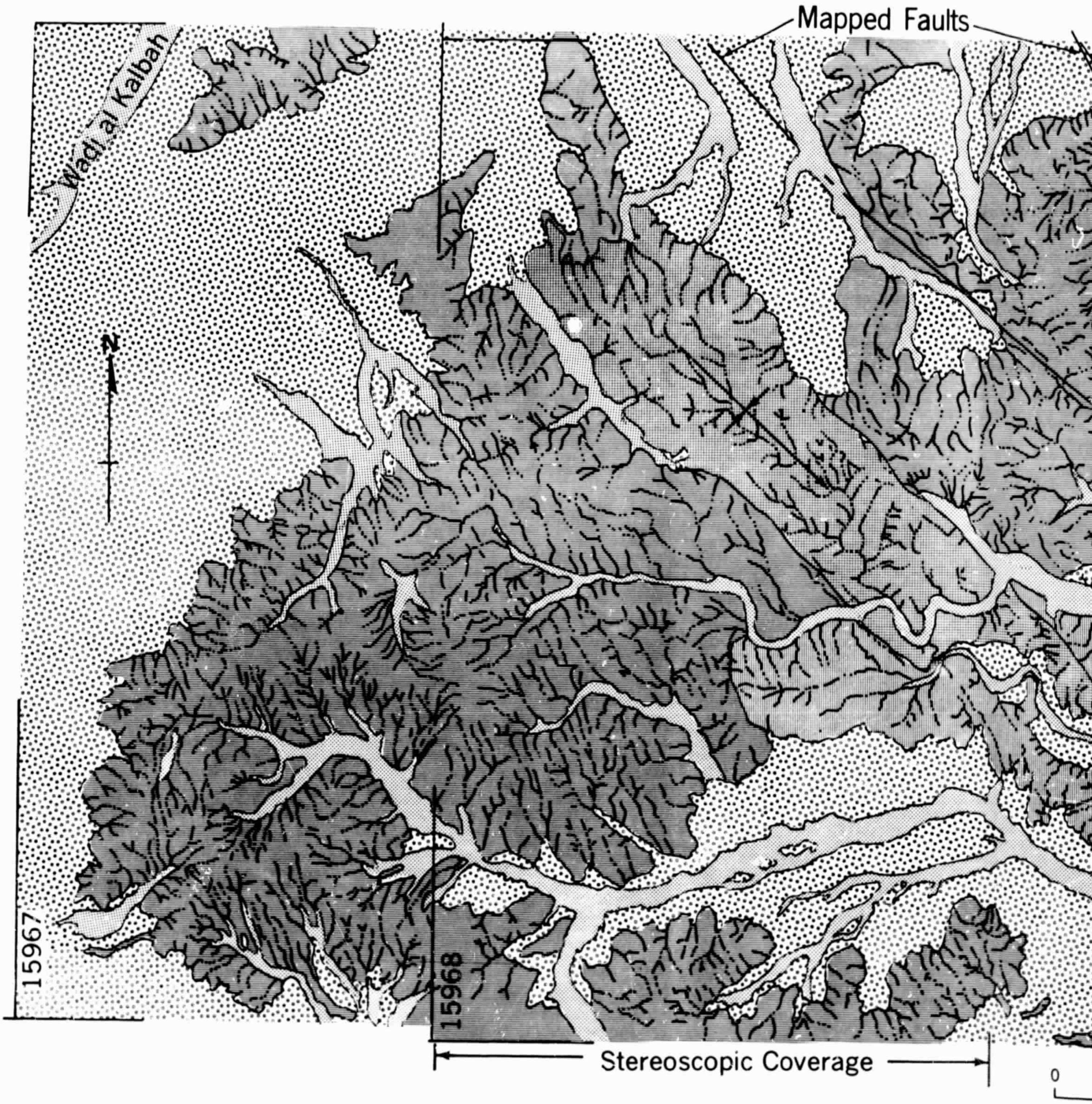

Fig

FOLDOUT FRAME

FOLDOUT FRAME

2

Figure 4. Area 2 Geologic Map – (Modified after Bramkamp, et al, 1963) – Based on Aircraft Photographs 15967 and 15968-WSA-96

The highly fractured, irregular, 16 square mile (42 km^2) body in the south-central part of the photo area is mapped by Brown, et al (1963) as probably massive, light colored, calc-alkalic grainte devoid of dikes (gm?). The sharp discordance between the granite and adjoining greenstone is best recognized along the extreme southeast and southwestern contacts. These characteristics, and its size, identify this igneous body as a stock. The drainage system developed on the granite forms a rectangular pattern strongly controlled by a well-developed fracture system. The generally short, straight tributaries which drain into the main arteries appear to be controlled by both linear texture, apparently expressing foliation in the granite body, and subsidiary fractures.

The generally light-toned rocks in the western corners of the photo area are described by Brown (1963) as red to salmon-pink, calc-alkalic massive granite which tends to be porphyritic, having large microcline or orthoclase crystals in the border facies. This granite type generally occurs as large, discordant intrusives. The fractured southwest outcrop exhibits a discordant contact with the greenstone on the northeast, but the remainder of the contact is covered by alluvial deposits. The granite in the northwest photo area is generally ill-defined on photo 9354-WSA-59, and difficult to distinguish from the greenstone on the basis of both tone and texture. Most of the contact between these two lithologic units is hidden by alluvial cover.

The lighter-toned unit in the extreme northeast is mapped as a probable red or pink, alkalic to peralkalic granite or syenite (gp?) of Precambrian age, which commonly contains accessory fluorite, riebeckite and aegirine. This lithology is generally restricted to circular plugs, stocks and ring dikes. However, the limited area covered by photo 9353-WSA-59 prevents delineation of gross structure. The contact with the greenstone is locally visibly discordant, but is more commonly covered by alluvial sediments. This unit appears to be fractured in part, but insufficient outcrop is visible to determine the configuration of the drainage system.

The majority of this photo area, which is topographically higher and darker in tone, is mapped as greenstone (gd), which is a generalized lithologic unit including andesite, diabase, slate and conglomerate. Its structure is generally obscure, and within the photo area, the unit is locally cut by light colored dikes. From tone, texture and weathering characteristics, this unit can be subdivided on the 1:60,000 scale. Because of local gradational contacts. however, any subdivision of this unit should best be confined to areas where stereoscopic coverage is available. The linear west-northwest topographic trend developed across the central portion of the photo area is the eroded remnant of a tightly compressed flexure. The steeply dipping strata which can be locally measured (Figure 5) provide an indication of the magnitude of the compressional forces. The

PRECEDING PAGE BLANK NOT FILMED

discordance of the granite body clearly indicates that flexural forces predate the intrusive.

An apparent anomalous relationship exists in the area of interest: the granites, which as a group are usually highly resistant to weathering, are generally topographically lower than the intruded greenstone. Several alternative models can be developed to account for this condition, but field data would be required to evaluate these photo interpretations.

Maximum resolution determined in areas of high tonal contrast and linearity, such as in areas where light-toned dikes cut darker greenstone, is measured to be :0 feet (6 meters). In areas of moderate contrast, however, such as on granite surfaces, maximum resolution is only 30 feet (9 meters).

Interpretation of 1:250,000 Index Mosaic 39

Index mosaic 39 of the western shield area, Saudi Arabia, includes the one degree area between 26 and 27 degrees north latitude and 36 and 37 degrees east longitude. The land areas consist predominantly of igneous and metamorphic Precambrian shield rocks which are locally overlain by Quaternary alluvial and eolian sediments. Near the Red Sea coast, and in Wadi Abu Masarib, the presence of local marine Tertiary (Tra?) and Quaternary (Qt) terrace-forming deposits indicates that many of the present low coastal and near-coastal areas were submerged during late Tertiary and Quaternary time (Brown, et al, 1963). The occurrence of distinct terrace levels at 10 feet (3 meters), 65 feet (12 meters) and 95 feet (30 meters) indicate at least three major periods of Quaternary epeiorogenic movement. Each of the major terrace levels described in the literature parallels the modern coast line and can be readily recognized, superimposed on the coastal terrace deposits. In addition, several less distinct terrace levels were locally developed which represent additional minor pauses in uplift.

The area covered by this mosaic is cut by an extensive subparallel fault system trending northwest from the southeast corner of the mosaic (Brown, et al, 1963). These faults appear to be a part of the wrench fault system dominated by the left lateral Najd fault described by Brown and Jackson (1960). Despite the extent of the faulting, however, only minor and local horizontal displacement can be confirmed on the index mosaic. The difficulty of recognizing displacement apparently results from parallelism of the faults and pre-fault structures, especially schistosity. The last movement on this fault system evidently occurred during late Paleozoic time, for overlying Permian rocks in the east are not disturbed. The Arabian fault zone, forming the east side of the Red Sea rift, lies below the coastal pediment and has apparently not been influenced by the Precambrian structural trends dominant on the Arabian shield. This faulting controls the

general straightness of the modern coast line seen in the mosaic area. Although movement along the total Najd zone has been negligible since Paleozoic time, the westernmost extension apparently was locally effected by the rifting mechanism during Tertiary time, and provided a pre-existing zone of weakness to control the limits of the present wadi Abu Masarib graben. The present Miocene evaporites and corals in this graben indicate that it formed an elongate gulf during Miocene and was subsequently raised above sea level with the taphrogenetic uplift of the Arabian highlands. Abdel-Gawad (1969) considers this wadi to be directly related to the Duwi shear zone in Egypt, but evidence to support the theory is not convincing.

In photo area 3, the resolution of the index mosaic is adequate to identify the limits of the four primary lithologies mapped in the area. In addition, the greenstone (gd) can be subdivided into two or possibly three units on the basis of tone and texture. The tight fold extending northwest from the irregular-shaped light colored granite (gm?) can be seen, but the magnitude of the structure and direction of limb dips can not be determined at this scale. Portions of the main drainage systems which just barely encroach on the north and south of the photo area can clearly be identified but the tributaries are generally below the resolution of the imagery. Many of the tributaries would be distinguishable, were the wadi bottom sediments the characteristic light tone typical of drainage systems in this region. Here, however, the alluvium is of local origin and retains the dark hue of the parent greenstone, producing little tonal contrast with the bedrock.

Resolution in the area of highest contrast, where the rectangular drainage is developed on the light colored granite, is approximately 155 feet (50 meters). In the greenstone area, the best resolution is 230 feet (75 meters). These generally low resolution figures are attributed to a lack of tonal contrast associated with linear features in the 100 to 125 foot (30 to 37.5 meter) range. In other parts of the mosaic where light toned linear drainage traverses dark lithologies, a maximum resolution of 115 feet (37.5 meters) is recognized.

Interpretation of the 1:1,000,000 Rectified Orbital Photography

On the rectified imagery, the irregular light colored granite intrusive can readily be identified by both tone and shape. The greenstone surrounding this granite is recognized by its characteristic dark tone, but sub-division of the unit is not possible. The other igneous lithologies recognized in the aircraft photo area are too minor a constituent of the area to be distinguished. When considered with areas contiguous to the immediate interest area, however, the lighter toned segments of the northeast and northwest corners can be recognized to be parts of the lighter colored units which are distinguishable from the greenstone and correlative with the units mapped by Brown, et al (1963).

The smallest feature determinable within the aircraft photo area is the light colored, sediment-filled wadi that trends along the northern border, and this, at its minimum recognizable width, is 735 feet (225 meters). Resolution falls off rapidly as tonal contrast becomes less, and meaningful quantitative comparisons can not be made. Increase in resolution on the unrectified color photograph enlargement is negligible in the immediate area of interest.

Comparison of the Various Scale Imagery

The 1:60,000 aircraft photographs yield by far the greatest detail, and exhibit an order of magnitude greater resolution over the photo mosaic. All geologic units shown can be identified in collaboration with the largest scale published maps, and in fact, the greenstone appears amenable to sub-division on the basis of photo tone and texture. In addition, a tight fold can be recognized and dips locally mapped. The small areal coverage of the individual photographs, however, prohibits the recognition of regional geologic inter-relationships.

Resolution at the 1:250,000 scale of the index mosaic is adequate to distinguish the main lithologic units mapped on the 1:500,000 scale in the immediate 115 square mile (300 km^2) study area. In addition, the greenstone appears to consist of two distinct units based on texture and tonal changes. The tightly folded flexure is evident, but dip direction can not be determined for the limbs. The mosaic does, however, make it possible to integrate the immediate area of interest into the shield complex, and in addition, to relate the Precambrian and lower Paleozoic structural trends to the Tertiary-Quaternary Red Sea rifting.

The inter-relationships of the rift and older shield structure, discussed earlier in relation to the index mosaic, are recognizable at the 1:1,000,000 scale. In addition, the increased area included in the synoptic view permits the integration of the one degree photo index area into the much larger tectonic system. For example, the proximity of extensive Cenozoic volcanics, which are probably genetically related to the Red Sea rifting (Cloos, 1939, et al) [less than 15 miles (24 km) east of the northern part of the mosaic area] can only be recognized in the larger field of view provided by the orbital imagery. For a more detailed discussion of the significance of the volcanics, the reader is referred to the Area 4 description.

An additional geologic relationship of regional extent that is visible only on the orbital photographs involves the family of igneous intrusions to which those shown on the air photos belong. Even casual study of the orbital photograph shows more than a dozen light colored bodies resembling the individual intrusions studied. However, only a few of these are shown on the

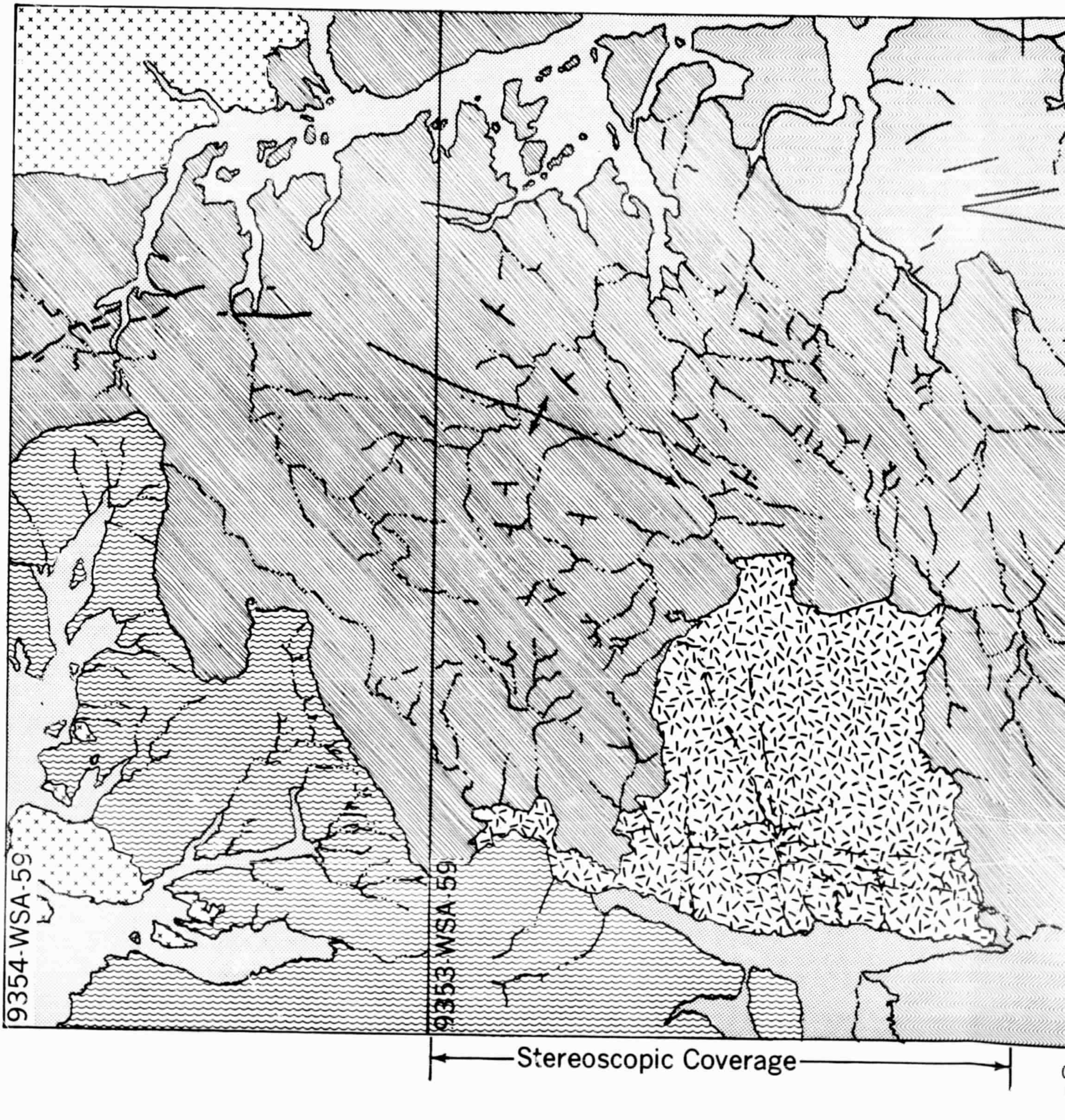
9354-WSA-59
9353-WSA-59
Stereoscopic Coverage

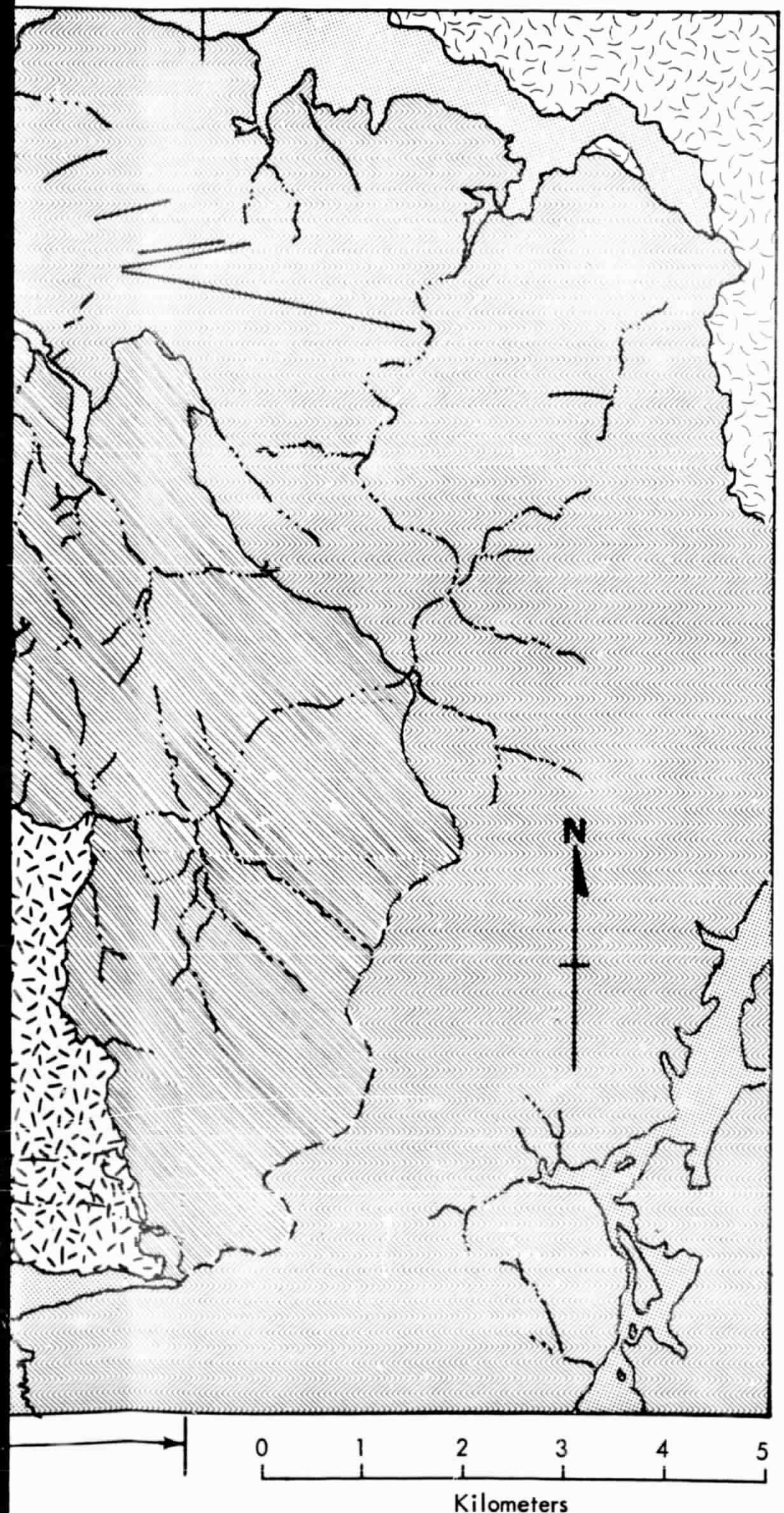

LEGEND

Quaternary: Gravel, sand, silt and clay, undiferentiated (Qu)

Precambrian: Granite or syenite, alkalic to perakalic (gp)

Precambrian: Granite, calc-alkalic, light-colored (gm)

Precambrian: Granite, calc-alkalic, pink (gr)

Precambrian: Greenstone, dark member (gd_1)

Greenstone, light toned folded member (gd_2)

Greenstone, lower member (upper surfaces removed by erosion), weathers distinctively (gd_3)

Dike

Strike and direction of dip

Plunging anticline

FOLDOUT FRAME

2

Figure 5. Area 3 Geologic Map – (Modified after Brown, et al, 1963) – Based on Aircraft Photographs 9353 and 9354-WSA-59

1:2,000,000 scale map (Anon., 1963) as peralkaline granite (gp), with the rest being mapped as granite gneiss (gg). The similarity of size, shape and tone among these bodies visible on the orbital photo suggests a closer relation than is apparent from the geologic map. Furthermore, several features in the Egyptian part of the Arabo-Nubian shield that closely resemble these igneous intrusions are recognized on the synoptic photograph. Whether these are in fact similar intrusions can not be determined solely on photographic evidence. The Nubian highlands have been a mineral-producing area for thousands of years (Flawn, 1966, pp. 73-100) and a similarity between the Egyptian and Saudi Arabian intrusions might be economically significant. Thus, if a systematic mineral search were being made in Saudi Arabia concentrating on igneous contacts, the use of an orbital photograph could suggest a larger number of prospective intrusions than would the published map. It should be noted that possible relations of this sort, involving the geology of two different countries, is very difficult to do with geological maps or air photos because of differences in scale, quality of mapping, dates and types and availability of photography, and similar problems. The Gemini photo used here, however, shows the whole area simultaneously with comparable scale and sun angle as well as usable resolution.

AIRCRAFT PHOTO AREA 4

Area 4 consists of overlapping photo pair 13581 and 13582-WSA-81, and was initially selected on photo index 41 to study the visibility of lithologic contacts on various scale photography. This photo area is well suited to attain this objective, for it includes several very contrasting granite-basalt contacts as well as less distinctive, differentially weathered multi-basalt flow contacts.

Regional Geologic Setting

Stratigraphy—This photo pair covers a 115 square mile (300 km^2) area located about 30 miles (50 km) northeast of the Red Sea coastal city Umm Lajj. Based on the best available map (Brown, et al, 1963), the photo area consists of Precambrian granite-granite gneiss (gg) and schist (sc) basement rocks which are largely covered by basalt and/or andesite extrusives (QTb). The igneous eruptions were of such magnitude that only the highest topographic Precambrian areas now remain as steptoes in a sea of basic igneous flows.

Structure—The Precambrian rocks are a part of the stable Arabian shield, which, prior to Tertiary time, was an eastern projection of the Nubian shield of Africa. During Tertiary time, as discussed earlier, the Arabian shield was separated from Africa by Red Sea rifting. Many of the Tertiary extrusives which now overlie much of the western shield area are believed to be genetically

 PRECEDING PAGE BLANK NOT FILMED

associated with the rifting mechanism (Cloos, 1939; Gillmann, 1968; Rittmann, 1962, p. 261; et al).

Interpretation of the 1:60,000 Aircraft Photography

The area recorded by photographs 13581 and 13582-WSA-81 includes two basically contrasting lithologies. The light colored, topographically high, angular-irregular-shaped areas are igneous and metamorphic rocks typical of the Precambrian shield complex. The dark, topographically lower areas are basic lava flows which were extruded over the low shield surfaces during Tertiary, Quaternary and Recent time.

The massive-weathering, grey mountainous outcrops near the southwest corner of the photo area have been mapped by Brown, et al (1963) as Precambrian schist, and consist of sericite and chlorite schists which variably contain actinolite, tremolite, coarse biotite, hornblende and quartz; locally the schists are calcareous, graphitic and pyrite bearing. The massive weathering exhibited by this Petrologic unit is not characteristic, for schists are more commonly differentially eroded along foliation zones, which produces a lamellated surface structure (von Bandat, 1962, p. 149). The remaining Precambrian areas are mapped together as granite and granite gneiss (gg). This petrographic unit is a grey, medium-grained, hornblende-albite granite of the syntectonic type, and contains many inclusions and xenoliths; strain shadows in the quartz are characteristic. At the 1:60,000 scale, this unit can be readily sub-divided into a patterned unit (gg_2), which includes the four outcrops in the south, and a massive unit (gg_1) forming the three northern units (Figure 7). The characteristic lamellate weathering and drainage pattern exhibited by the southern unit appears to be controlled by foliation trends modified by local fracturing. The three northern light colored outcrops exhibit a widely spaced radial drainage pattern characteristic of massive units highly resistant to weathering (von Bandat, 1962, p. 126).

The topographically low intervening Precambrian areas were intermittently flooded by volcanic extrusives from the Tertiary to Recent time. These flows have been formally described by Brown, et al (1963) as commonly olivine-rich basalts and andesites which generally originated as fissure eruptions. Within the immediate photo area, however, the existence of over 50 volcanic craters and erosional cone remnants suggest that a substantial amount of the local extrusive materials is from these vents rather than from fissures.

At least three distinct major volcanic periods as well as several minor periods of eruption can be distinguished from superposition and weathering characteristics (Figure 7). The youngest (QTb_3) consists of black and dark grey multi-flow units which are so recent and unweathered that characteristic surface expressions

indicative of flow movement and solidification are still clearly preserved. These features include flow fronts, pahoehoe surfaces, pressure ridges (schollenrücken), tumuli (schollendome), collapse structures and cooling fractures among others. Where these surfaces are topographically low, they contain but a trace of the eolian sediments that would be anticipated in this tropical desert area. The difference in tone and surface texture between individual recent extrusive bodies may be due to weathering, but more likely, it is the result of different chemical and physical characteristics of the individual lavas. The intermediate extrusive unit (QTb_2) consists of dark grey to black volcanics on which nearly all the distinct flow features have been obscured or altered by weathering. Small topographically low areas formed by lava solidification fractures and local collapse and differential weathering contain light-toned deposits of probable eolian origin. These small discrete deposits are ubiquitous over this volcanic unit, and produce a speckled tonal pattern which is one of the basic characteristics of the unit. Near the center of the photo area this unit is obviously overlain by younger flows. The oldest volcanic unit (QTb_1) on the photographs is a medium grey, smooth-weathering flow which has been largely covered by younger eruptives. In the photo area, it is most commonly present as volcanic cones protruding through the younger flows.

Maximum resolution determined in areas of high tonal contrast and linearity, such as solidification fractures on the dark young extrusive layers, is measured to be 20 feet (6 meters). In areas of moderate contrast, however, such as the areas of massive-weathering Precambrian intrusives, no linear feature smaller than 40 feet (12 meters) can be resolved.

Interpretation of 1:250,000 Index Mosaic 41

Index mosaic 41 of the western shield area, Saudi Arabia, includes the 1 degree area bounded by the 25 and 26 degree north latitude and 37 and 38 degree east longitude graticules. It includes areas of the Precambrian Arabian shield that are locally covered by Tertiary to Recent extrusives. On the west, the shield complex is bordered by Red Sea coastal deposits.

The area included in the 1:60,000 photo pair study area is readily distinguished on the mosaic. The three mapped Precambrian units can be identified, but at this small scale it is difficult to distinguish the tone and weathering characteristics of the massive-weathering granite (gg_1) from the schist (sc). The dark flows which surround the steptoes are readily identifiable both by their characteristic dark tone and the presence of volcanic cones and their associated flows. Of the three extrusive units mapped at the 1:60,000 scale, only the younger two can be identified within the photo area, and dated in respect to each other. On the mosaic, however, the flows can be followed west-northwest to where all three

individual volcanic units can be recognized and age related. The western-most volcano cluster in the immediate interest area appears to be crudely aligned in a north-northwest direction, roughly parallel to the Red Sea coast. Although this alignment is admittedly poor, it does suggest a rift-volcanic relationship as first proposed by Cloos (1939).

Within the mosaic area, it is recognized that the volcanics are a part of a large irregular-shaped volcanic field covering approximately 925 square miles (2400 km^2). In addition, the specific igneous and metamorphic lithologies which dominate the area of the aircraft photo are, in fact, relatively minor constituents of the total shield complex included in the one degree mosaic area.

Maximum resolution is developed where light toned linear features cut dark basalt flows as on the 1:60,000 scale, and is measured to be 115 feet (35 meters) on the mosaic. In areas of lower contrast, resolution is reduced to only 155 feet (50 meters).

Interpretation of the 1:1,000,000 Rectified Orbital Photography

Each of the steptoes seen on the 1:60,000 photography can be easily identified on the rectified orbital photograph by a combination of shape, color and position in the photo area. Although texture and weathering characteristics can not be determined from this imagery, a definite color change from a light grey to a darker grey is visible across the granite-granite gneiss (gg) - schist (sc) contact. These units are even more clearly contrasted on the unrectified satellite color photography. The dark grey and black crab-shaped feature is typical of lava flows covering areas topographically lower than their source. Within the 1:60,000 photo area, subtle color changes suggest a varied volcanic lithology but subdivisions can not be delineated on the orbital imagery alone. On another, more nearly vertical, orbital photograph, S66-54895 (Figure 6), the two younger flows can be easily distinguished from each other, but their relative ages would be extremely difficult to determine. The great magnitude of the volcanic field of which the immediate interest area is an integral part, is well shown on the orbital photography. In addition, on the synoptic coverage, it is observed that this relatively large volcanic area is only one of the smaller parts of a large volcanic area which overlies much of the shield complex located within 200 miles (320 km) of the northern Red Sea coast.

Resolution in the high tonal contrast areas northwest of the volcanic flows, where light toned alluvium of wadi Murykhat overlies shield rocks, is determined in collaboration with the index mosaic to be approximately 625 feet (190 meters). The resolution falls off so rapidly with decrease in tonal contrast that meaningful quantitative comparisons can not be made. Resolution on the near-vertical orbital

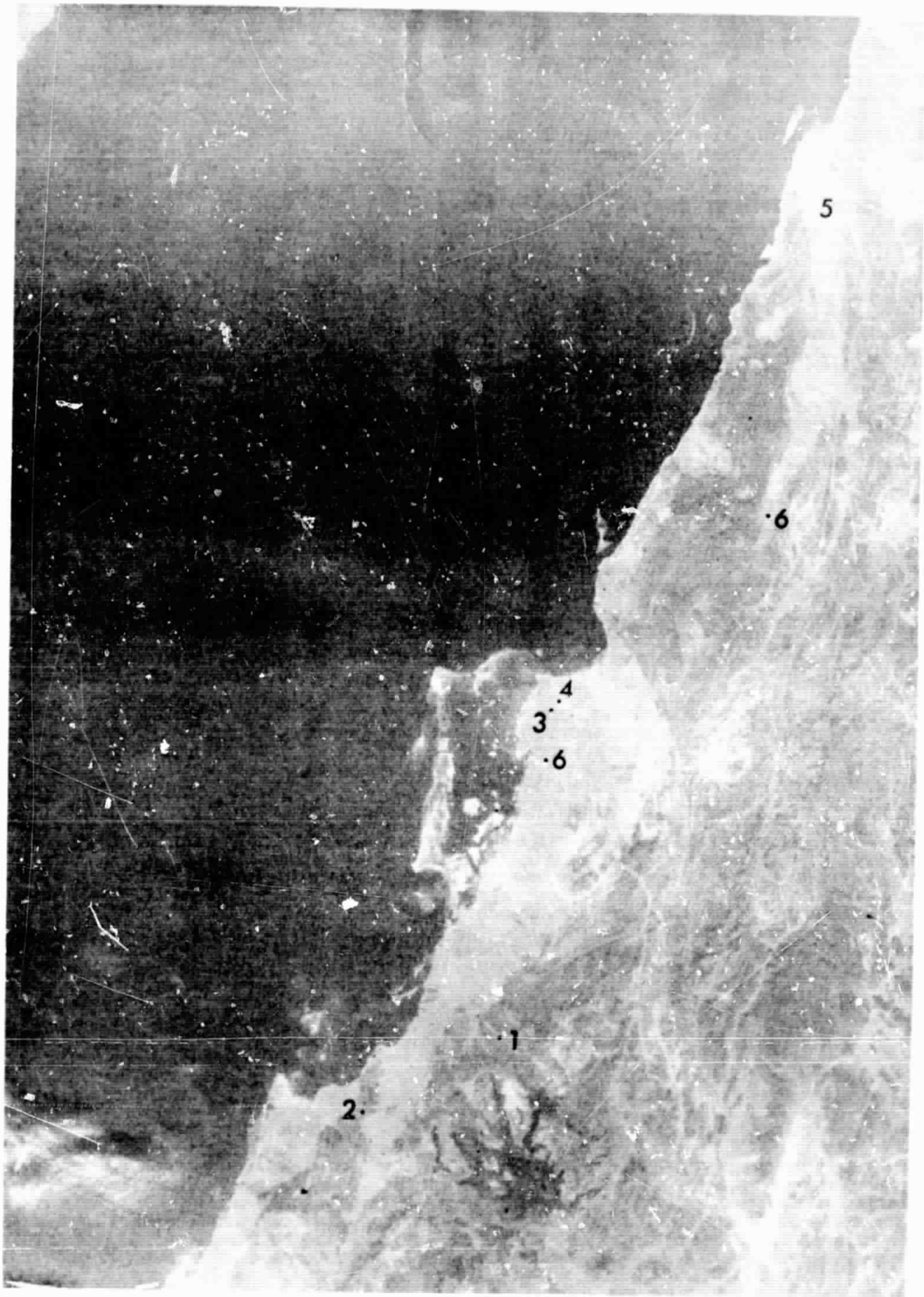

Figure 6. NASA Photograph S66-54895. Scale Approximately 1:1,300,000. Localities Cited in Text: 1 - wadi Murykhat; 2 - wadi Nikbah; 3 - Jabal Karkuma; 4 - wadi al Hamd; 5 - Abu Masarib Shear Zone; 6 - Quaternary Terrace Deposit.

photo, measured in the wadi Nikbah area west of the spider-shaped extrusion, is approximately 460 feet (140 meters). This drainage unit is below the resolution of photo S66-54644 and its rectified image. Surface feature recognition capability thus is significantly increased as verticality is approached, as would be expected.

Comparison of the Various Scale Imagery

The 1:60,000 scale aircraft photographs yield by far the greatest total detail. All the major geologically mapped lithologies can be identified in collaboration with published maps, and in fact, these units can be further subdivided on the basis of distinctive tonal and textural differences. The small areal coverage of individual photographs, however, makes it impossible to recognize the geologic relations of the small area in a regional context.

Resolution at the 1:250,000 scale of the photo index mosaic is adequate to distinguish the lithology recorded on the largest scale published geologic map (1:500,000). In addition, the major subdivisions visible on the aircraft imagery (Figure 7) can be identified, but the relative age determination of the two older volcanic units is difficult. The mosaic does, however, make it possible to relate the immediate interest area to the regional framework. The immediate study area, for example, is recognized as part of an area of extensive volcanic activity, where extrusions overlie a fractured basement complex.

The resolution of the rectified earth-orbital photograph is adequate to identify the aircraft photo area within the crab-shaped volcanic field, and to distinguish the individual geologic units mapped at 1:500,000 scale. In addition, the one degree area of the index mosaic can be viewed as a part of a much larger tectonic system. The extensive flows in the mosaic area, for example, form only one of several such flows within 200 miles (320 km) of the northern Red Sea coast, and the overall igneous associations suggest a genetic relationship to the mechanism responsible for the Red Sea rifting.

An additional scale-resolution comparison of this study area is possible using near vertical photograph S66-54895, which has a scale of approximately 1:1,300,000 (Figure 6). The total area included is considerably smaller than that of photograph S66-54644, for as verticality is approached, the area included in an aerial photograph becomes smaller and distortion of the terrestrial surface features caused by the oblique photo angle become less. The ideal, of course, is vertical photography.

The advantages of color synoptic photography over black and white photo mosaics and rectified imagery is clearly illustrated in the Red Sea coastal areas. Where Quaternary sediments have the widest lateral distribution in the S66-54895 photo

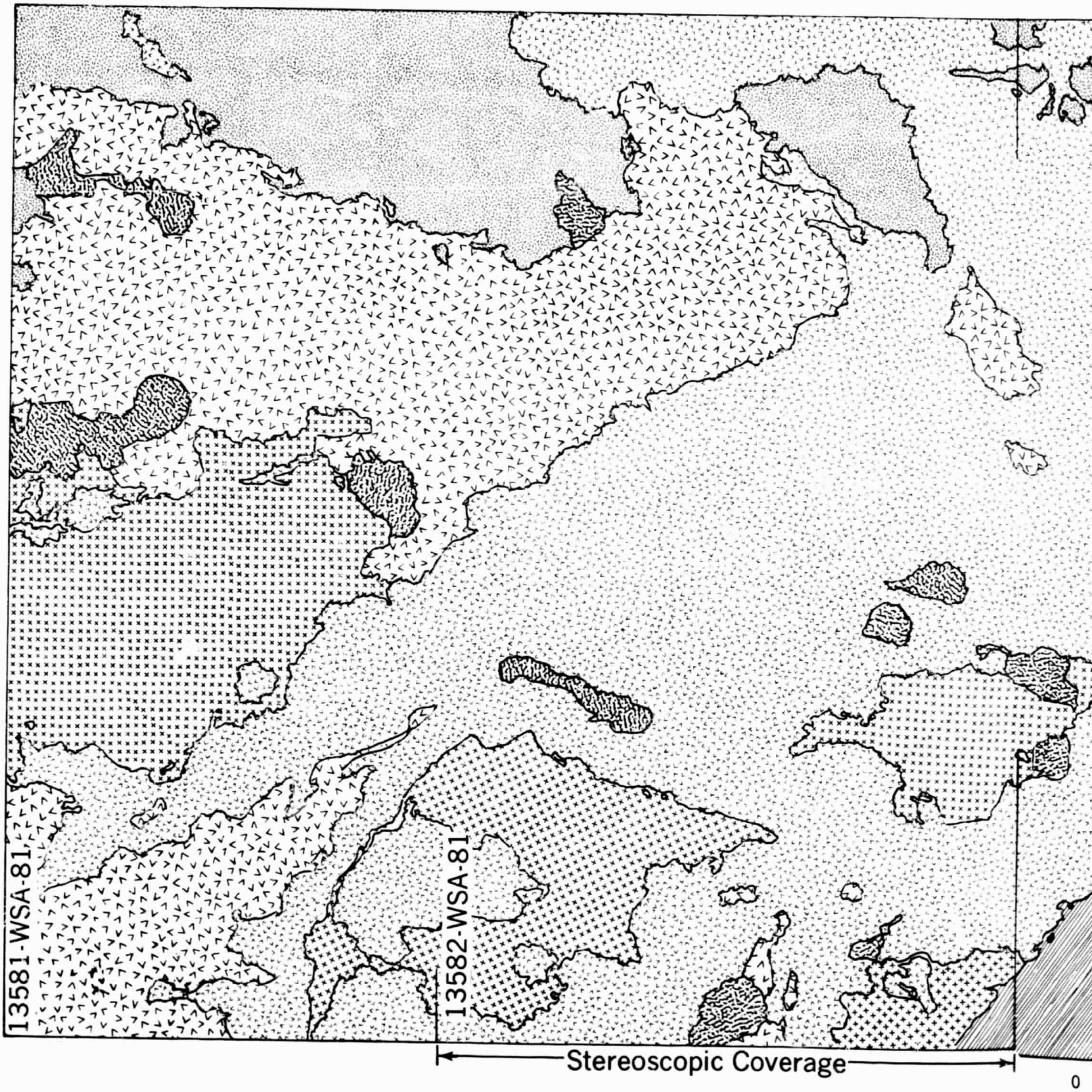

FOLDOUT FRAME

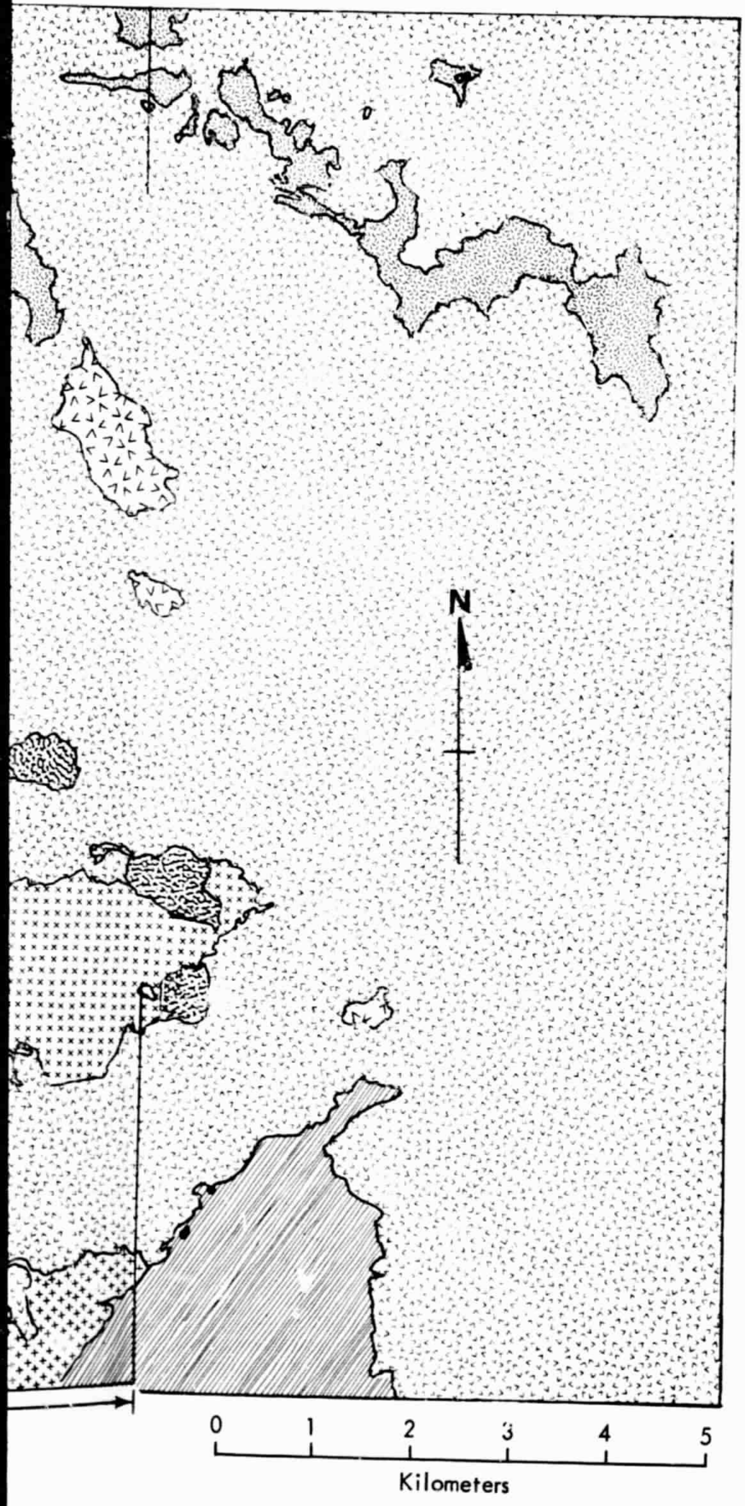

LEGEND

Quaternary: Basalt and andesite; youngest flows (QTb_3)

Basalt and andesite; intermediate age flows (QTb_2)

Basalt and andesite; oldest flows (QTb_1)

Precambrian: Granite and granite gneiss, patterned member (gg_2)

Granite and granite-gneiss, massive member (gg_1)

Precambrian: Schist (sc)

FOLDOUT FRAME

2

Figure 7. Area 4 Geologic Map – (Modified after Brown et al, 1963) – Based on Aircraft Photographs 13581 and 13582-WSA-81

area (Figure 6), distinct outlines of Quaternary units can be identified in collaboration with the 1:500,000 mapping. The terrace-forming unit mapped by Brown, et al. (1963), includes the entire terrace suite, consisting of distinct benches at three levels (Qt). The terrace deposits mapped in the Jabal Karkuma area can be clearly identified on the basis of their distinctive grey-tan color which contrasts with the contiguous tan wadi aluvium and saline mud flat sediments (Qu). Approximately 10 miles (16 km) south of wadi al Hamd, across a straight sharp contact, the lithology is a distinctly lighter hue and suggests that at least two distinct benches can be distinguished in this immediate area.

Northward along the Red Sea coast, additional terrace deposits can be identified at the western end of the Abu Masarib shear zone. To the southeast, however, the mapped Quaternary strata are shown as undifferentiated sediments (Qu), which locally surrounds isolated saline and near-shore marine calcareous and argillaceous deposits (Tra?). Judging from color and the knowledge that the wadi was below sea level during Tertiary time, it seems probable that additional terrace deposits can be identified locally near the graben walls and forming the southern-most 10 miles (16 km) of this structural depression. (For a discussion of the structural relationships, see the Area 4 description.)

AIRCRAFT PHOTO AREA 5

Area 5 includes the sidelapping aircraft photo pair 15107-WSA-90 and 15140-WSA-91. It was initially selected (on index mosaic 57) because of the north-south trending oval structure which occupies the center of the overlapped pair and to determine its distinctiveness on various scale imagery.

Regional Geologic Setting

Stratigraphy—This photo pair includes a 145 square mile (375 km^2) area located approximately 26 miles (42 km) east-northeast of the Red Sea port city Yanbu al Bahr. Based on the best available published map of the area (Brown, et al., 1963) the rocks forming the concentric walls of the oval consist of Precambrian granite and granite gneiss (gg). This lithology consists of grey, medium grained, hornblend-albite granite and granite gneiss of the syntectonic type, and generally contains many inclusions and xenoliths. The constituent quartz characteristically exhibits strain shadows. The northeast and northwest flanks of this structure are in contact with a light colored calc-alkalic granite (gm). Within the 15140-WSA-91 photo area, the oval structure abuts a grey-black, commonly gneissic diorite on the southwest and is fault separated from a greenstone (gd) on the southeast. This latter lithology is a generalized unit which locally includes andesite, diabase, slate and/or conglomerate. All of these petrologic units are of Precambrian age.

Along the main drainage courses, the eroded basement is commonly covered by wadi alluvium (Qu).

Structure—Photo Area 5 is part of the Arabian shield. During Precambrian time, the complex shield area passed through several orogenic and erosional cycles, as indicated by the contorted, intruded and metamorphosed sediments, but since the start of the Paleozoic era, it has been comparatively stable. Structural movements occurring during Phanerozoic time were primarily epeirogenic, and are recorded in the sedimentary sequences of the Interior homocline — generally in the form of regional unconformities (Powers, et al, 1966).

Interpretation of the 1:60,000 Aircraft Photography

The most distinctive feature of this sidelapping photo pair is a 6 × 8 mile (10 × 13 km) elliptical structure located near the center of the photo area. Its rim rocks are closely parallel and breached by the local ephemeral drainage system; wadi Talhah, for example, cuts the northern rim and then progresses seaward through gaps in the southern and western flanks. The closely spaced, nearly concentric, locally fractured rim walls at first observation appear similar to the dome described in Area 1, however, the contiguous occurrence of a massive crystalline lithology, as well as the near-vertical nature of the "strata", indicate definitely that the structure is not sedimentary. The bed-like appearance is most likely the result of differential erosion controlled by foliation, as illustrated in standard photogeology texts (Tator, 1960, Miller, 1961, et al), and is indicative of metasediments. The elliptical ring is mapped as granite and granite-gneiss (gg), a lithology illustrated by von Bandat (1962, p. 128). In his Colorado type area, however, there is no preponderance of eroded linears in either the granite or granite-gneiss, so the structural associations most likely contribute strongly to the greater accentuation of the foliation layering in Area 5. Foliation dip direction measured in the field by Brown, et al (1963) is inward from the rim, which would further eliminate the possibility of the feature being an eroded domal uplift. Alternative interpretations which consider the inward dipping foliations would include meteorite impact cratering, ring dike intrusion and the presence of a steep-sided metasedimentary syncline. Of these possibilities, the dip of the foliations is too steep for an impact crater (Beals, et al, 1963), and the individual resistant bed-like layers appear too thin for the structure to be a ring dike (Billings, 1954, pp. 312-317). Thus, a steep-sided syncline model appears to best fit the evidence immediately available.

The crystalline area immediately to the north of the structure has been geologically mapped by Brown, et al (1963) as being the same as the ellipse area. Erosional patterns of this homogeneous massive outcrop, however, indicate no obvious foliation-controlled drainage. Thus it appears that these rocks may be

appreciably different from each other, and are mapped accordingly at the 1:60,000 scale (Figure 8). At the 1:500,000 scale, however, a great enough similarity exists to warrant mapping as a single unit. The light colored calc-alcaline granite (gm) mapped at the northeast and northwest corners of Area 5 can easily be distinguished from the gg_1 member, for its color is lighter, and a drainage change occurs across the contact, going from dendritic on the gg_1 surface to a more complex dendritic-pectinate pattern (von Bandat, 1962, p. 41). This, of course, is a clear indication of the differing weathering and erosional characteristics which would be expected between two contrasting rock types.

A highly fractured diorite (di) which is locally intruded by generally northeast trending diabase (?) dikes, flanks the oval-shaped structure on the southwest. The angular or trellis drainage pattern developed on this petrologic unit is controlled by a complex fracture pattern. The dark sub-circular ring feature at the extreme south of the photo area is interpreted to be the eroded remnant of a basic extrusion even though it is mapped by Brown, et al (1963) as granite-granite gneiss. Its position adjacent to the diorite may also suggest a genetic relationship to the diabase (?) dikes which intrude that unit.

The triangular area of greenstone (gd) in the extreme southeast photo area is fault-separated from the adjacent intrusives (?) and granite/granite-diorite (gg_2) lithology. This generalized lithologic unit includes andesite, diabase, slate and conglomerate, but in the immediate area, it appears to have photographic characteristics most indicative of a locally fractured diabase.

Maximum resolution determined at high contrast diorite-linear alluvium contacts is measured to be 20 feet (16 meters). In areas of moderate contrast, however, the resolution is only 30 feet (9 meters).

Interpretation of 1:250,000 Index Mosaic 57

Index mosaic 57 of the western shield area, Saudi Arabia includes the one degree area bounded by the 24 and 25 degree north latitude and 38 to 39 degree east longitude graticules. Geologically it includes a part of the complex Arabian shield which is bordered on the west by Red Sea coastal deposits.

The large elliptical structure that dominates the 1:60,000 photo area is clearly visible on the index mosaic, but at the smaller scale it appears to form part of a larger 25 mile (40 km) diameter sub-circular igneous body. This larger structure is distinguished from the adjacent lithology on the mosaic, by its darker color, massive weathering texture, and a relative paucity of major fracturing. As mapped by Brown, et al (1963), it consists of granites which are locally gneissic (gm). The structural significance of the elliptic ring can still not be readily identified even when placed in its regional context.

Each of the major rock units recognized on the aircraft photographs (Figure 8) can be identified at the 1:250,000 scale, but much of the fine tectural detail is lost. The major units of the drainage system can be equally well distinguished at the smaller scale but the nature of the 3rd and 4th order tributaries, which is so different across the dark and light colored granite contacts, is clearly below the resolution of the index mosaic.

One drainage feature of note in the immediate interest area is a classic example of incipient stream piracy. Wadi Qarrah originally eroded headward through the western and northern rims of the elliptical ring, and formed the trunk of the system draining the central area of the large sub-circular igneous structure. Subsequently, wadi Thamai, a roughly parallel drainage channel located approximately 10 miles (16 km) to the south, eroded headward into the southern portion of the oval rim and continued northward to intersect the head water channel of wadi Qarrah (together with which it now forms wadi Talhah). As noted on the aircraft photographs, some of the drainage still traverses the west rim, but this is probably only during times of highest water flow associated with flash floods. The great preponderance of southward drainage indicates that in the very near geologic future, wadi Qarrah will be completely beheaded.

Maximum resolution in the linear high contrast areas of the mosaic is measured to be 155 feet (50 meters). In areas of moderate contrast, resolution is reduced about 50 percent to 230 feet (75 meters). These generally low resolution figures are attributed to a lack of high contrast linear features in the area, within the 100 to 125 foot (30 to 40 meter) range.

Interpretation of the 1:1,000,000 Rectified Orbital Photography

Within the aircraft photo area, arcuate portions of the east and west rims of the oval ring can be recognized, but the total symmetry of the structure is below the limits of resolution. The three main trunk wadis previously discussed, as well as the indications of stream piracy, can be recognized, but their detailed interrelationships at this scale can not be identified. Despite the inherent advantages of color imagery (Carter, 1969) recognition of additional geologic features in the immediate area of interest on the unrectified film is negligible.

Resolution in the high contrast areas is determined in combination with the index mosaic and is measured to be approximately 570 feet (175 meters). Resolution degrades rapidly with decrease in photo tonal contrast, and additional meaningful quantitative comparisons can not be made. The resolution in this area is appreciably better than in similar-sized areas to the north on the rectified imagery because it is closer to the nadir of photo S66-54644.

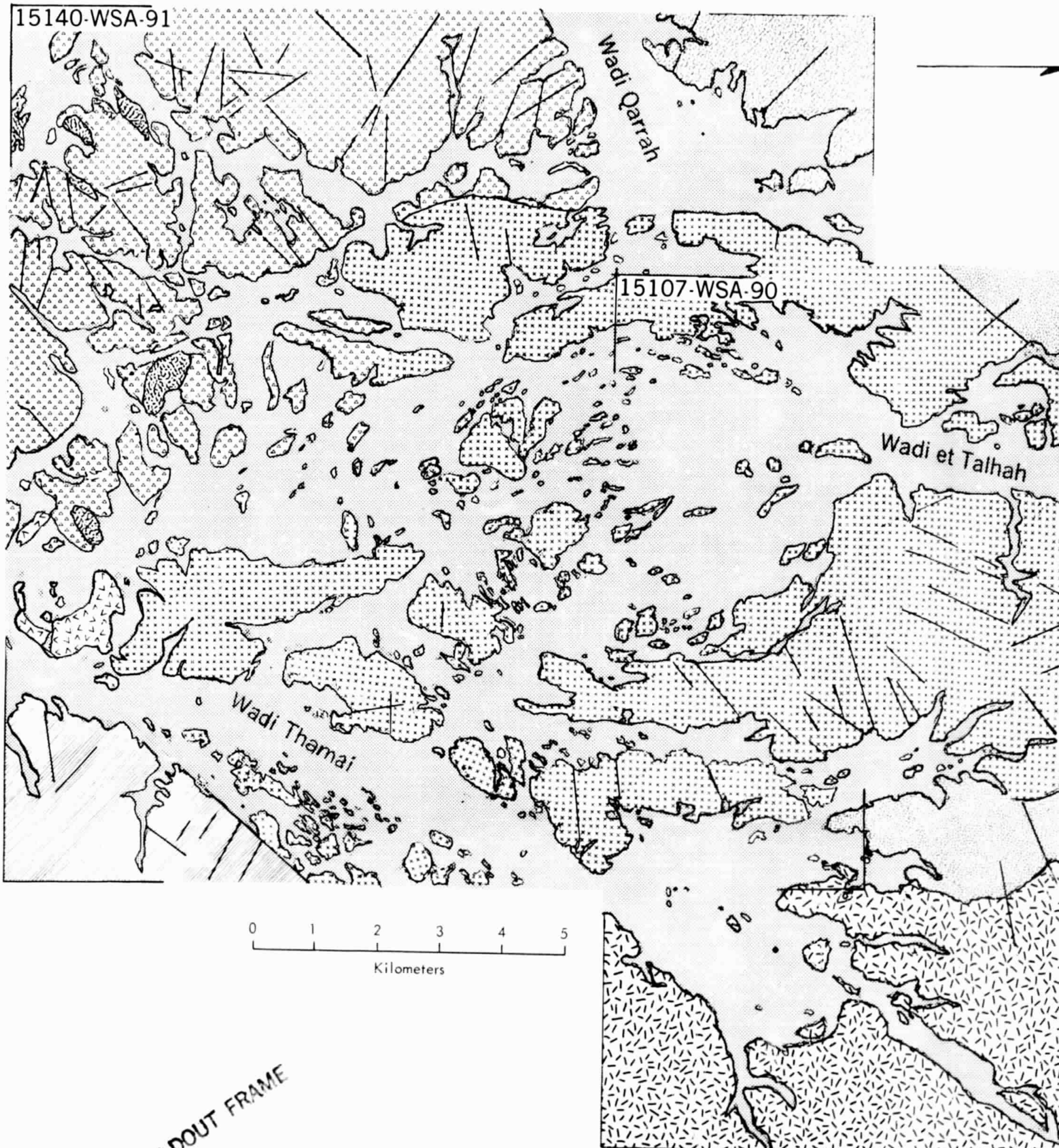

FOLDOUT FRAME

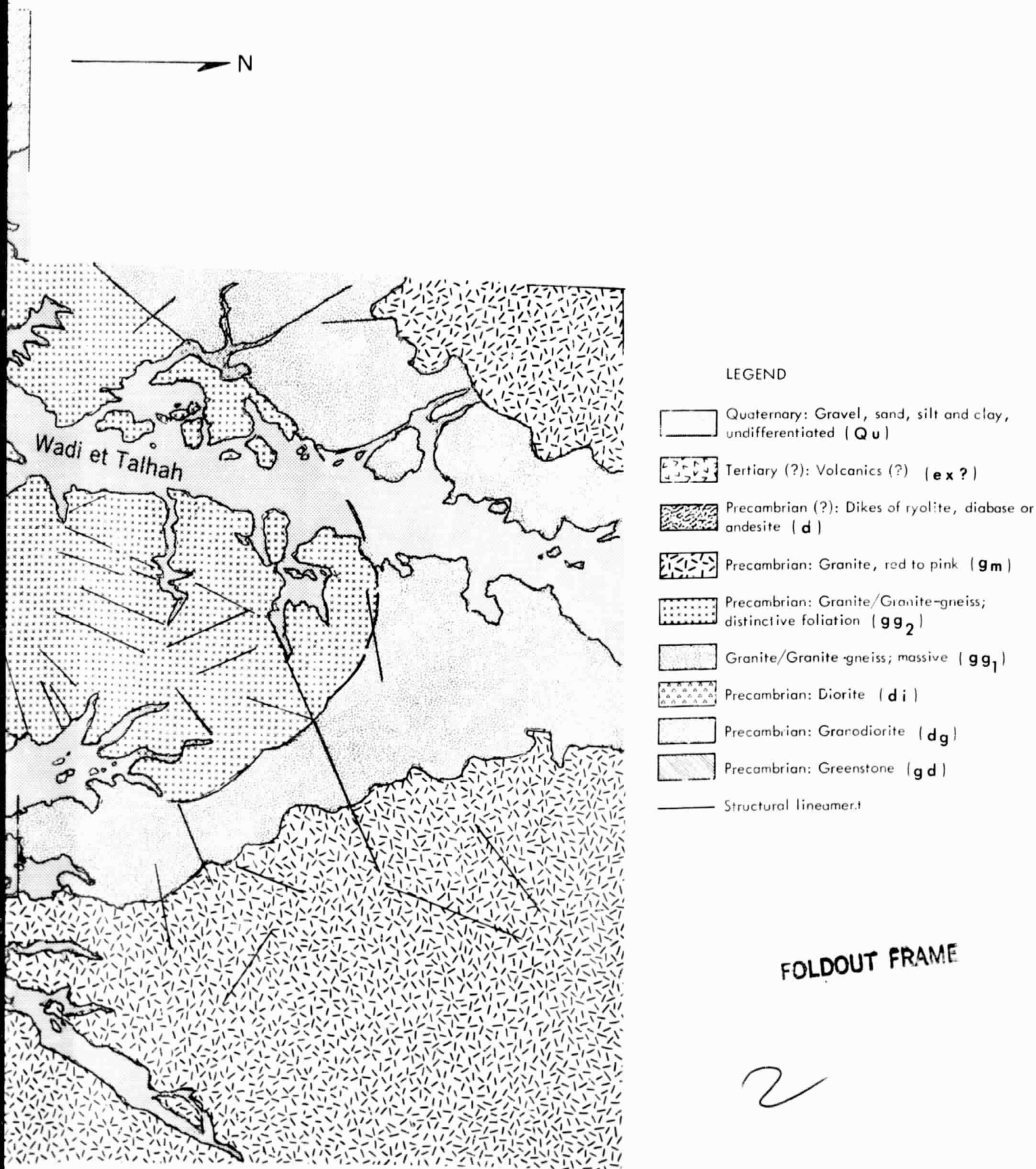

2

Figure 8. Area 5 Geologic Map – (Modified after Brown, et al, 1963) – Based on Aircraft Photographs 15140-WSA-91 and 15107-WSA-90

Comparison of the Various Scale Imagery

The 1:60,000 aircraft photographs yield the greatest detail. All the major lithologies can be differentiated in collaboration with published maps, and relatively small drainage changes across lithologic contacts can easily be distinguished. The main disadvantage of the large scale photography in the immediate area is the difficulty of placing the area of interest in regional perspective.

Resolution of the 1:250,000 mosaic is adequate to distinguish major lithology on the basis of tone and to a lesser extent surface texture. Recognition of the major segments of the regional drainage systems is possible, but significant changes in the third and fourth order tributaries is below the limits of resolution. The mosaic has the distinct advantage of permitting specific areas to be readily placed in the regional context.

Resolution of the rectified orbital photograph and the unrectified film is only adequate for the recognition of the larger drainage units and marginal differentiation between the largest lithologic contrasts. This imagery provides regional coverage and permits identification of many significant large trends. For the study of relatively small distinctive features having no apparent regional interrelationships, however, the advantages of earth orbital photography are negligible.

SUMMARY AND CONCLUSIONS

Five types of imagery at different scales were compared in order to evaluate the utility of each in providing geologic information.

Of the photography studied in this investigation, the 1:60,000 aircraft photographs yield by far the greatest geologic detail. Resolution, determined in areas of maximum apparent contrast, averages approximately 22 feet (6.5 meters), and falls off to about 35 feet (10 meters) where tonal contrast is less (Table 1). Lack of ground control prevented the more reliable determination of effective resolution data. This resolution is adequate to identify fifth order drainage tributaries, and to permit recognition of much greater geologic detail than is illustrated on the largest scale geologic maps (1:500,000). The smallest lithologic units identified are 20 feet (6 meters) wide, light-toned dikes which cut the greenstone in Area 3, and similar dimension light-toned deposits of probable eolian origin, on dark lava surfaces (QTb_2) of Area 4. In addition to the attractive resolution characteristics, this photography is also available with stereoscopic coverage which is a major asset in doing detailed geologic interpretations.

While the 1:60,000 photography provides the greatest geologic detail, the total area covered by a single standard photograph, slightly greater than 100 square

Table 1

Comparative Resolution
(Determined in Areas of High/Moderate Tonal Contrast)

Scale	1:60,000	1:250,000	1:1,000,000
Area			
1	30 ft (9 m)/40 ft (12 m)	115 ft (35 m)/155 ft (50 m)	1.5 mi (2.4 km)
2	20 ft (6 m)/30 ft (9 m)	115 ft (35 m)/155 ft (50 m)	975 ft (300 m)
3	20 ft (6 m)/30 ft (9 m)	155 ft (50 m)/230 ft (75 m)	735 ft (225 m)
4	20 ft (6 m)/40 ft (12 m)	115 ft (35 m)/155 ft (50 m)	625 ft (190 m)
5	20 ft (6 m)/30 ft (9 m)	155 ft (50 m)/230 ft (75 m)	570 ft (175 m)

miles (260 km^2), is generally inadequate to provide any significant knowledge concerning regional lithologic distribution or structure.

The 1:250,000 index mosaics provide much wider areal coverage, but resolution is conversely significantly reduced. Within the selected interest areas, maximum resolution, determined in the highest contrast areas, averaged approximately 130 feet (42 meters). This is adequate to identify third and even some fourth order tributaries in areas of high tonal contrast. In lower tonal contrast areas, resolution is reduced to about 185 feet (60 meters). The smallest lithologic units recognized at this scale the irregular-shaped, probable eolian deposits on lava flows found in Area 4 on index 41, and these have a minimum lateral coverage of 155 feet (50 meters). If it were not for the high tonal contrast, these smaller deposits could not be identified.

The much wider coverage provided by the mosaics enhances recognition of regional geologic relationships. Each of the specific interest areas studied on the aircraft photography can be readily identified, and viewed at this scale, each can be seen in the lithologic and tectonic framework of a 5,000 square mile (13,000 km^2) region. Thus, certain volcanic areas can be seen in their entirety and studied in respect to regional structure, and each of the unique geologic features selected for this study can be seen in relation to its regional surroundings.

For regional geological evaluation, however, the index mosaic has several inherent undesirable characteristics. The nature of index mosaic construction requires that the border containing the identification number of each 1:60,000 photo area be clearly indicated. This produces the rectangular mosaic pattern superimposed on the regional geology. If the mosaic had been constructed with geologic usage as its primary objective, half of the two-third overlap coverage could be omitted, but the basic problem would still exist. Second, changes in light effects produced by the time difference between adjacent flight lines produces different tonal characteristics between individual flight lines and makes differentiation of surface units more difficult.

The 1:1,000,000 scale photograph rectified from Gemini 11 photograph S66-54644 provides a broad view for the study of regional tectonics and generalized lithology distribution. Resolution of this imagery is much poorer than that of the mosaic, and because of the mechanics of construction, is also not uniform over the entire picture. Maximum resolution determined in the five areas studied became progressively poorer toward the horizon, and ranged from 570 feet (175 meters) in Area 5, nearest nadir, to 1.5 miles (2.4 km) in Area 1. Because of this resolution degradation caused by rectification, regional geologic interpretations are best made directly on enlarged, nonrectified color photographs. The rectified imagery can then be best used to correlate the data for plotting onto a standard map projection.

The enlarged unrectified color orbital photography provides the best format for small scale regional geologic mapping. Although resolution is variable and low, the synoptic color photography is adequate for recognition of most of the lithologic units mapped at a 1:500,000 scale; locally it actually appears to be even more detailed than the published maps.

The large area included within a single orbital photograph provides a global view which can be especially useful in generalized lithologic and structural mapping. Small geologic features become muted at the small scale, and only the major relationships can be recognized. The lower resolution can thus be an advantage for certain studies. This characteristic is particularly useful in studying regional tectonics related to orogenesis and plate tectonics. In addition, regional structure can be viewed together with related regional lithologic units to determine structural and volcanic relationships, and also to determine areas potentially prospective for mineralization.

The Nimbus HRIR imagery, at a scale smaller than 1:15,000,000, is suited for viewing intercontinental tectonic relationships. On the image investigated, all the major structural provinces of the Central and Western Arabian peninsula, as defined by Powers, et al (1966), and even the eastern provinces, which are

distorted at the edge of the photo, can be identified. In addition, the parallelism of the Red Sea coasts, which has long been used as evidence to support both incipient sea floor spreading and graben faulting as the mechanism responsible for the origin of the Red Sea, is clearly visible. Imagery at this scale is thus helpful in understanding intercontinental tectonic relationships, but having maximum resolution of only five miles (8 km) it is doubtful if any significant new geologic data can be obtained.

All interpretations made from orbital imagery should, of course, be supplemented with field data, published geologic literature and larger scale photography as available.

This study clearly demonstrates that each type of imagery is uniquely suited for investigation of a specific class of geologic problem. For study of small geologic detail and construction of precise maps, aerial photography is unexcelled. Mosaics permit extrapolation of inferences from individual photographs to larger areas, but with loss of detail. Orbital color photography appears to combine many advantages of mosaics and air photographs, for despite its relatively low ground resolution, it is clearly valuable for studying regions of sub-continental size. When rectified, resolution on synoptic photos is degraded, but the resultant near vertical projection enables more accurate correlation of data between the unrectified photography and standard geologic formats. Orbital scan-type imagery, with very low ground resolution, may not be directly useful in geologic research, but provides a useful view of continental and intercontinental relationships. The various methods of remote sensing discussed are thus complementary, rather than competitive, and can advantageously be utilized together in regional geologic investigations.

REFERENCES

Abdel-Gawad, M., 1969, New evidence of transcurrent movements in Red Sea area and petroleum implications: Am. Assn. of Petrol. Geologists Bul., v. 53/7, p. 1466-1479.

________, 1970, Interpretation of satellite photographs of the Red Sea and Gulf of Aden: in Phil. Trans. of the Royal Soc. of London, A. Math. and Phys. Sci., v. 267, No. 1181, p. 41-48.

Amsbury, D. L., 1969, Geological comparison of spacecraft and aircraft photographs of the Potrillo mountains, New Mexico and Franklin mountains, Texas: Proceedings of the Sixth International Symposium on Remote Sensing of Environment, Center for Remote Sensing Information and Analysis, the University of Michigan, Ann Arbor, Michigan, v. 1, p. 493-515.

Anon., 1963, Geologic map of the Arabian peninsula: U.S. Geological Survey miscellaneous geologic investigations map I-270 A, scale 1:2,000,000.

Beals, C. S., Innes, M. J. S. and Rottenberg, J. A., 1963, Fossil meteorite craters: in Middlehurst, B. M. and Kuiper, G. P., editors, The moon meteorites and planets: University of Chicago press, Chicago, p. 235-284.

Billings, M. P., 1954, Structural geology: 2nd ed, Prentice-Hall, Inc., New York, 514 p.

Bramkamp, R. A., Brown, G. E., Holm, D. A. and Layne, N. M., Jr., 1963, Geology of the wadi as Sirhan quadrangle, Saudi Arabia: U.S. Geological Survey miscellaneous geologic investigations map I-200 A, scale 1:500,000.

Brown, G. F., 1970, Eastern margin of the Red Sea and coastal structures in Saudi Arabia: in Phil. Trans. of the Royal Soc. of London, A. Math. and Phys. Sci., v. 267, No. 1181, p. 75-87.

Brown, G. F. and Jackson, R. O., 1960, The Arabian shield: in Simonen, A. and Kouvo, F. A. O., eds., Int'l. Geologic Cong., Rpt. of the 21st session Norden, Pt. 9, Proceedings of Sec. 9, Precambrian stratigraphy and correlations: Det Berlingske Bogtrykkeri, Copenhagen, p. 69-77.

Brown, G. F., Jackson, R. O., Bogue, R. G. and Elberg, E. L., Jr., 1963, Geology of the northwestern Hijaz quadrangle, Saudi Arabia: U.S. Geological Survey miscellaneous geologic investigations map I-204 A, scale 1:500,000.

Carter, W. D., 1968, Some uses of space photography in earth resources surveys: in Smith, J. T., ed, Manual of color photography: Am. Soc. of Photogrammetry, Falls Church, Va., p. 398-399.

Cherrix, G. T. and Allison, L. J., 1969, The high resolution infrared radiometer (HRIR) experiment: in Sabatini, R. R., ed., The Nimbus users guide: Goddard Space Flight Center, Greenbelt, Md., p. 29-65.

Choubert, G., General Co-ordinator, 1968, International tectonic map of Africa, Sheet No. 3: Assn. of African Geological Surveys, U.N. Educational, Scientific and Cultural Orgn., Paris, scale 1:5,000,000.

Cloos, H., 1939, Hebung, Spaltung, Vulkanismus: Geologische Rundschau, Bd. 30, Zwischenheft 4 A, p. 406-527.

Cotton, C. A., 1952, Volcanoes as land forms, 2nd ed.: Whitcombe and Tombs Ltd., Christchurch, N.Z., 416 p.

Dalrymple, R. G., 1970, Cartographic applications of orbital photography: NASA, Goddard Space Flight Center publication X-644-70-110, Greenbelt, Md., 95 p.

Datet, P., Marchesseau, J., Million, R. and Motti, E., 1970, Mineral occurrences related to stratigraphy and tectonics in Tertiary sediments near Umm Lajj, eastern Red Sea area, Saudi Arabia: in Phil. Trans. of the Royal Soc. of London, A. Math. and Phys. Sci., v. 267, No. 1181, p. 99-106.

Dubertret, L., Coordinator, 1963, Geological map of Africa, sheet No. 3: Assn. of African Geological Surveys, U.N. Educational, Scientific and Cultural Orgn., Paris, scale 1:5,000,000.

________, 1970, Review of structural geology of the Red Sea and surrounding areas: in Phil. Trans. of the Royal Soc. of London, A. Math. and Phys. Sci., v. 267, No. 1181, p. 9-20.

Easterbrook, D. J., 1969, Principles of Geomorphology: McGraw Hill book company, New York, 462 p.

Feldman, S., Harris, S. A. and Fairbridge, R. W., 1968, Drainage patterns: in Fairbridge, R. W. ed., the Encyclopedia of geomorphology: Reinhold book Corp., New York, p. 284-291.

Flawn, P. T., 1966, Mineral resources: Rand McNally and Co., Chicago, 406 p.

Furon, R., 1963, The geology of Africa: Hafner publishing Co., New York, 377 p.

Gillmann, M., 1968, Primary results of a geological and geophysical reconnaissance of the Jizan coastal plain in Saudi Arabia: in Proceedings of the Second Regional Symposium, Soc. of Petrol. Eng. of A.I.M.E., Saudi Arabia Sec., Dhahran, p. 189-212.

Holm, D. A., 1968, Sand dunes: in Fairbridge, R. W., ed., The encyclopedia of geomorphology: Reinhold book Corp., New York, p. 973-979.

Hunter, G. T. and Bird, S. J. G., 1970, Critical terrain analysis: Photogrammetric Eng., v. 36, No. 9, p. 939-952.

Lowman, P. D., Jr., 1964, A review of photography of the earth from sounding rockets and satellites: NASA Tech. note, TDN-1865, Greenbelt, Md., 25 p.

________, 1969, Geologic orbital photography: Experience from the Gemini program: Photogrammetria, v. 24, p. 77-106.

MacKallor, J. A., 1968, A Gemini mosaic along the thirty-second degree of latitude from Baja California to central Texas: Interagency report NASA-114, Prepared by the U.S. Geological Survey, Wash., D.C., 11 p.

Merifield, P. M., Cronin, J., Foshee, L. L., Gawarecki, S. J., Neal, J. T., Stephenson, R. E., Stone, R. O. and Williams, R. S., Jr., 1969, Satellite imagery of the earth: Photogrammetric Eng., v. 35, No. 7, p. 654-668.

Miller, V. C., 1961, Photogeology: McGraw Hill book Co., inc., New York, 248 p.

Nordberg, W., 1970, Remote sensing of the atmosphere: in, Shapiro, K. A., coordinator, Remote sensing of the environment: Lecture notes for short course presented at U.C.L.A., chapter 4.

Powers, R. W., Ramirez, L. F., Redmond, C. C. and Elberg, E. L., Jr., 1966, Geology of the Arabian peninsula, sedimentary geology of Saudi Arabia: U.S. Geological Survey Prof. paper 560 D, 147 p.

Rittmann, A., 1962, Volcanoes and their activity: Interscience publishers, a Div. of John Wiley and Sons, New York, 305 p.

Said, R., 1962, The geology of Egypt: Elsevier Publishing Co., New York, 377 p.

Smith, H. T. U., 1963, Eolian geomorphology, wind direction and climatic change in north Africa: Air Force Cambridge Research Laboratories contract AF 19-(628) -298, final report (mimeographed), Amherst, Mass., 49 p.

Stearns, H. T., 1966, Geology of the State of Hawaii: Pacific books, Palo Alto, California, 266 p.

Tator, B. A., 1960, Photo interpretation in geology: in Colwell, R. N., ed., Manual of photographic interpretation: Am. Soc. of Photogrammetry, Washington, D.C., p. 169-332.

von Bandat, H. F., 1962, Aerogeology: Gulf Publishing Co., Houston, 350 p.

Wobber, F. J., 1967, Space photography: a new tool for the sedimentologist: Sedimentology, v. 9, p. 265-317.